

**INVESTIGATION OF ENZYMATIC HYDROLYSIS PROCESS TO VALORIZE
WASTE MUSSEL SHELLS**

by

© Thi-Hong-Xuan Nguyen, B. Eng.

A Thesis Submitted to the School of Graduate Studies

in partial fulfillment of the requirements of the degree of

Master of Engineering

Process Engineering

Faculty of Engineering & Applied Science

Memorial University of Newfoundland

October 2021

St. John's, Newfoundland, Canada

Abstract

Blue mussels (*Mytilus edulis*) are the most common mussel harvested with high value nutritional compounds including proteins, vitamins (C, A, and B12), and minerals (iron and calcium). Blue mussels are filter feeders eating plankton from the water. Mussel farming is more sustainable form of aquaculture as fish meal, chemicals (antibiotics and additives) are not required and the risk of pathogens escaping into the coastal ecosystems is minimal. The worldwide aquaculture and processing of mussels is rapidly increasing and blue mussels are Canada's top shellfish aquaculture product produced in every province in Atlantic Canada, as well as in Quebec and British Columbia. By-products from mussel aquaculture and processing, such as processed mussel shells, unmarketable and broken mussels, make up a significant waste stream from this industry and are currently difficult to valorize. Waste mussel shells are a potential source of bio-calcium carbonate and proteins. Protein enzymatic hydrolysis, a process where protein macromolecules are hydrolyzed to amino acids and peptides of smaller size. The process is a simple, effective, and environmentally friendly means of valorizing waste mussel shells, producing two product streams: mussel shells without residual meat and non-toxic hydrolysate. This study includes a review of literature on valorizations of waste mussel shells for the source of bio-calcium carbonate and proteins. The review shows the lack of kinetic studies for enzymatic hydrolysis of mussels, required for any scale up to a commercial process. In this study, mussel meat is removed from whole mussels by using enzymatic hydrolysis technology. The process is carried out using a food grade enzyme, Multifect PR 6L, and tap water at neutral pH, with no pH control, and a temperature 50°C. To determine the rate of hydrolysis, the degree of

digested meat (DM) is used in this study instead of the degree of hydrolysis (DH). The enzyme and substrate concentrations were varied to determine the impact of these factors on the final digested meat and rate of reaction. The fraction of digested meat (or degree of shell cleaning) varied from 0.57 g/g_{meat} to 0.94 g/g_{meat} depending on the enzyme and substrate (meat) concentrations. Soluble protein concentration of the obtained hydrolysates was also analyzed. After evaluating a number of reaction rate mechanisms, the first-order model is suggested as the best model to describe the enzymatic hydrolysis of whole raw mussels. The soluble protein concentration in the resulting hydrolysate increases with the increases in the amount of digested meat.

Acknowledgments

The research presented in this thesis could not have been performed without the funding provided by the Ocean Frontier Institute (OFI), Sunrise Fish Farms Inc., the Memorial University of Newfoundland School of Graduate Studies, and the Memorial University of Newfoundland Faculty of Engineering & Applied Science.

I would like to thank, first and foremost, my supervisor for this project, Dr. Kelly Hawboldt. Her continued support and guidance in this project were imperative in guiding the work of this thesis and helping me to become a better researcher, and for that, I have extreme gratitude towards her. Furthermore, I would like to thank Dr. Hawboldt for providing a fellowship and encouraging me to pursue research in this field; without her support, I would certainly not come to Canada and do my Master degree. Her advice and moral support throughout this thesis were important in helping me complete this degree. I would also like to extend gratitude towards Dr. Laura Halfyard for providing mussels for experiments.

I would also like to thank my family for their continued support throughout this thesis. Without their inspiration and love for higher education and engineering fields, I would never have found my love for this field, and I am proud to be able to complete their dream.

Table of Contents

| | |
|--|-----|
| Abstract | i |
| Acknowledgments | iii |
| Table of Contents | iv |
| List of Figures | vii |
| List of Tables | ix |
| List of Abbreviations | x |
| CHAPTER 1 – INTRODUCTION & OVERVIEW | 12 |
| 1.1 Background | 12 |
| 1.2 Research Objective and Scope | 13 |
| 1.3 Thesis Organization | 14 |
| REFERENCES | 15 |
| CHAPTER 2 – LITERATURE REVIEW | 16 |
| 2.1 Introduction | 16 |
| 2.2 Properties of waste mussel shells | 18 |
| 2.3 Potential applications of waste mussel shells | 24 |
| 2.3.1 Calcium supplement | 25 |
| 2.3.2 Soil amendment | 25 |

| | | |
|-------|--|----|
| 2.3.3 | Wastewater treatment..... | 27 |
| 2.3.4 | Filler | 31 |
| 2.3.5 | Construction | 33 |
| 2.3.6 | Catalyst | 34 |
| 2.3.7 | Hydroxyapatite production | 35 |
| 2.4 | Protein enzymatic hydrolysis in by-products of fish processing | 40 |
| 2.5 | Kinetic models of protein enzymatic hydrolysis in by-products of fish processing | 45 |
| 2.6 | Conclusions..... | 55 |
| | REFERENCES | 57 |
| | CHAPTER 3 – MATERIALS & EXPERIMENTS | 67 |
| 3.1 | Experimental | 67 |
| 3.1.1 | Materials | 67 |
| 3.1.2 | Equipment | 69 |
| 3.1.3 | Enzymatic hydrolysis of whole raw mussels using Multifect PR 6L enzyme 70 | |
| 3.1.4 | Degree of digested meat..... | 72 |
| 3.2 | Kinetic models for enzymatic hydrolysis of fish protein:..... | 75 |
| 3.3 | Characterizations analysis - Solubilized protein concentration of hydrolysate | 79 |

| | |
|--|-----|
| REFERENCES | 80 |
| CHAPTER 4 – RESULTS AND DISCUSSION | 82 |
| 4.1 Effect of the initial enzyme and mussel age (or substrate concentration) on hydrolysis of raw marketable mussel..... | 82 |
| 4.2 Model validation for the enzymatic hydrolysis of whole raw marketable size mussels | 86 |
| 4.2.1 The Peleg equation (1988) | 87 |
| 4.2.2 The exponential equation | 90 |
| 4.2.3 First-order kinetic equation | 94 |
| 4.3 Protein concentration of hydrolysate obtained from mussel meat hydrolysis ... | 99 |
| REFERENCES | 101 |
| CHAPTER 5 – CONCLUSIONS AND RECOMMENDATIONS | 102 |
| 5.1 Conclusions:..... | 102 |
| 5.2 Future Recommendations: | 103 |

List of Figures

Error! Reference source not found.....Error!

Bookmark not defined.

Error! Reference source not found.....Error!

Bookmark not defined.

Error! Reference source not found.....Error! Bookmark not defined.

Error! Reference source not found.....Error!

Bookmark not defined.

Error! Reference source not found.....Error! Bookmark not defined.

List of Abbreviations

| | | |
|-------|---|----------------------------------|
| EPA | – | Eicosapentaenoic acid |
| DHA | – | Docosahexaenoic acid)), |
| AMD | – | Acid mine drainage |
| BET | – | Brunauer-Emmett-Teller |
| CMS | – | Calcined mussel shells |
| CSTR | – | Continuous stirred tank reactor |
| DAP | – | Di-ammonium hydrogen phosphate |
| DH | – | Degree of enzymatic hydrolysis |
| DM | – | Degree of digested meat |
| DHA | – | Docosahexaenoic acid |
| EDTA | – | Ethylenediaminetetraacetic acid |
| EPA | – | Eicosapentaenoic acid |
| HA | – | Hydroxyapatite |
| HV | – | The Vickers Pyramid Number |
| IR | – | Infrared spectroscopy |
| L-ARG | – | L-arginine |
| LDPE | – | Low-density polyethylene |
| MS | – | Mussel shell |
| NMR | – | Nuclear magnetic resonance |
| PAHs | – | Polycyclic aromatic hydrocarbons |
| PP | – | Polypropylene |

| | | |
|------|---|------------------------------|
| SEM | – | Scanning Electron Microscopy |
| TGA | – | Thermogravimetric Analysis |
| TNBS | – | Trinitrobenzenesulfonic acid |
| WMS | – | Waste mussel shells |
| WMS | – | Waste mussel shells |
| XRD | – | Powder X-ray Diffraction |

CHAPTER 1 – INTRODUCTION & OVERVIEW

1.1 Background

Mussel contains an array of nutritional compounds such as long-chain fatty acids (EPA (eicosapentaenoic acid) and DHA (docosahexaenoic acid)), vitamins (C and B12), and essential minerals (zinc and iron) [1]. Like other bivalves, mussel farming has a minimal ecological impact and reduces the pressure on wild-caught fishing [2]. The worldwide production of mussels has grown steadily and reached 2.2 million tonnes in 2018 [3]. Mussel is one of the most important shellfish aquaculture products in Canada. Mussels are farmed and produced mainly in Newfoundland and Labrador, Nova Scotia, Prince Edward Island, and Quebec.

Approximately 27% of the harvest is considered to be reject materials [4]. The growth in mussel aquaculture and processing has led to an increase in these rejects, including shells with meat removed (processed), unmarketable mussels, mussels with broken shells, and barnacle-fouled mussels [4]. Mussel shells are discarded with residual meat from both mussel aquaculture and processing, especially from the pre-cooked and ready-to-eat mussel production, such as frozen meat mussels, smoked mussels, and canned mussels. Waste mussel shells are primarily disposed of in landfills, representing an environmental burden and cost to the processor.

Mussel shell is a rich source of bio-CaCO₃, which can be used in several applications, including nutritional supplements, agriculture, plastic and paper production, water and wastewater treatment, catalyst industry, and hydroxyapatite production. The residual

mussel meat is also a rich source of proteins which can be used for low-level products such as fishmeal and animal supplement. Studies using enzymatic hydrolysis have shown the potential to obtain meat-free shells and protein hydrolysate. Protein enzymatic hydrolysis is an environment-friendly process due to mild reaction conditions and the potential for zero waste.

Previous research determined using a food-grade (and therefore relatively inexpensive) enzyme, Multifect PR 6L, to hydrolyze mussel meat showed the process was feasible [4,6]. These studies have investigated the type of enzyme, impact of salinity, as well as the reaction conditions (e.g., pH, temperature, etc.) [4],[5],[6]. In order to scale up, the rate and extent of hydrolysis is required. A rate of reaction model can describe and predict the impact reaction conditions (temperature, enzyme concentration, substrate concentration, etc.) and be used in process design. In addition, the quality of obtained hydrolysate needs to be analyzed to determine their potential in a further application and maximize the products from the enzymatic process.

This research investigates the rate of enzymatic hydrolysis to solubilize/remove the meat from the shell by varying the initial concentration of enzyme and substrate. Based on this data, a kinetic model is developed for scaling up and studying the impact of process parameters such as enzyme:substrate ratio. The obtained hydrolysate is analyzed for soluble protein content to determine its value.

1.2 Research Objective and Scope

The disposal of waste mussel shells is not only a burden on the environment but also in the loss of a valuable source of CaCO_3 and proteins. The utilization of waste mussel shells as a value added by-product is attractive. The potential application of mussel shells and mussel proteins was investigated in a number of studies. However, there is no work on the kinetic model of the hydrolysis process and subsequent separation of product streams.

The main objectives of this research are to investigate and determine the kinetic model of the meat removal process by using enzymatic hydrolysis, including:

- Examining factors affecting the enzymatic hydrolysis of whole raw mussel by varying the initial enzyme and substrate concentration.
- Develop a kinetic model describing and predicting the degree of digested meat during the hydrolysis period.
- Characterizations of mussel protein hydrolysate

1.3 Thesis Organization

The thesis is outlined in five chapters. Chapter one briefly introduces the background, the objectives, and the basic contents of the research work. The literature is reviewed in chapter two. In chapter three, the experimental works are described, including the characterization of enzymes and mussel meat and experimental method. The results and discussion are presented in chapter four. Chapter five contains a comprehensive conclusion and recommendation.

REFERENCES

- [1] S. Almonacid, J. Bustamante, R. Simpson, and M. Pinto, *Shellfish (Mussel) Processing and Components*. Elsevier Inc., 2015.
- [2] “Farmed Mussels.”
- [3] E. T. D. E. L. Aquaculture, *FAO Yearbook. Fishery and Aquaculture Statistics 2018/FAO annuaire. Statistiques des pêches et de l’aquaculture 2018/FAO anuario. Estadísticas de pesca y acuicultura 2018*. 2020.
- [4] A. S. Naik, L. Mora, and M. Hayes, “Characterisation of seasonal mytilus edulis by-products and generation of bioactive hydrolysates,” *Appl. Sci.*, vol. 10, no. 19, pp. 1–21, 2020.
- [5] J. N. Murphy, K. Hawboldt, and F. M. Kerton, “Enzymatic processing of mussel shells to produce biorenewable calcium carbonate in seawater,” *R. Soc. Chem.*, vol. 20, pp. 2913–2920, 2018.
- [6] V. M. Silva, K. J. Park, and M. D. Hubinger, “Optimization of the enzymatic hydrolysis of mussel meat,” *J. Food Sci.*, vol. 75, no. 1, 2010.

CHAPTER 2 – LITERATURE REVIEW

2.1 Introduction

World fish production has increased rapidly in the last ten years. In 2018, total world fisheries production was estimated at 178.5 million tonnes, an increase of 25.4 % from 2008, and the world capture production was 96.4 million tonnes, an increase of 5.4 %. World aquaculture production was 82.1 million tonnes in 2018, an increase of 37.3% from 2011 [1]. The aquaculture sector plays a key role in food production. However, the high demand for fishmeal and other aquaculture operating factors puts pressure on wild feed fish stocks, food resources, and the environment [2][3]. Harvesting mollusk, a filter-feeding species, is an environmentally sustainable form of aquaculture. The product provides high nutritional seafood for human consumption but with fewer environmental impacts than other types of aquaculture [4].

The global production of mollusks has grown steadily and accounts for almost 13.3% of total world fisheries production in 2018 [5]. By mass, oysters, clams, groups of squid, cuttlefishes, and octopuses dominate the world production of mollusks, followed by scallops and mussels, Figure 2 - 1 [1].

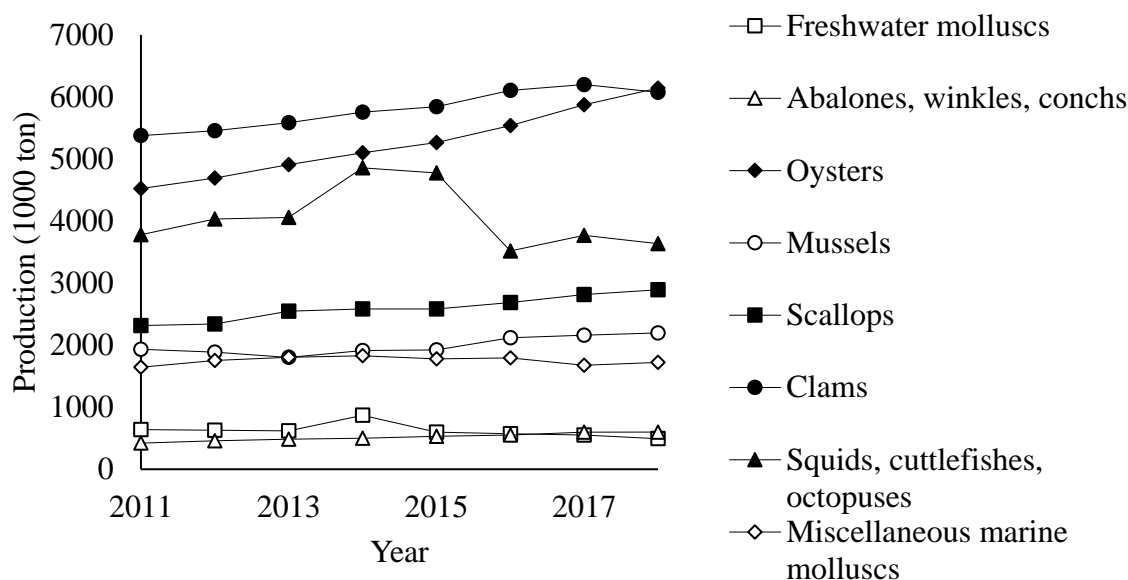


Figure 2 - 1: The world production of Mollusks [1]

Mussels, which account for 9.2 % of total mollusks production in 2018, contain high levels of nutritional compounds such as long-chain fatty acids EPA (eicosapentaenoic acid) and DHA (docosahexaenoic acid). Mussels are a source of vitamins C and B12 and essential minerals (zinc and iron) [6]. Mussel is an important shellfish aquaculture product in Canada, and farmed and produced mainly in Newfoundland and Labrador, Nova Scotia, Prince Edward Island, and Quebec [7]. Eastern Blue mussel (*Mytilus edulis*), Western Blue mussel (*Mytilus trossulus*), Gallo/Mediterranean mussel (*Mytilus galloprovincialis*) are the three main types of Canada's farmed mussels [7]. In 2015, 25,800 tonnes of mussels were produced in Canada, an annual average farm-gate value of \$ 44.7 million [7].

Mussel processing can be as simple as harvesting, sorting, and cleaning for the fresh mussel market or a more intensive process with additional steaming, meat removal, and freezing for frozen and canned mussel markets. Regardless of the process there is associated by-

product which is underutilized. By-products of the mussel industry include byssus threads, undersized mussels, damaged mussels, and processed mussel shells with residual meat [8]. Waste mussel shells (WMS) can account for up to 70-75 wt.% of the total harvested weight and includes WMS with meat attached, unmarketable, and damaged mussels [9][10]. The organic matter (meat) must be treated and disposed of properly which in turn adds to costs, particularly for undersized or damaged mussel disposal. In addition, to the cost, WMS represent a loss of valuable products in the form of the shell and residual meat.

Mussel shell (MS) is mainly composed of CaCO_3 (as calcite or aragonite in the protein matrix) [8]. The source of the bulk of current commercial CaCO_3 is mined in the form of limestone [11]. Mined CaCO_3 has high costs related to its production, including energy consumption, CO_2 emissions, and other environmental impacts [11]. Residual meat of WMS is a promising source of protein that could be utilized for animal food or fishmeal. The utilization of WMS as a source of bio- CaCO_3 and proteins not only reduces the burden of WMS on the environment but also mitigates the impact of mining of CaCO_3 [11]. This would also decrease the costs associated with waste treatment and add high-value by-products.

2.2 Properties of waste mussel shells

MS roughly accounts for 31-33% of the total mussel weight [12]. MS is mainly composed of minerals and a small amount of organic compound such as proteins, β -chitin, and glycoproteins [8][10][13][14]. XRD analysis indicates that the chemical composition of MS is predominantly CaCO_3 (95 wt.%), Table 2- 1 [15].

Table 2- 1: MS mineral composition (heat treated 135°C, 32 min) [15]

| Components | wt.% |
|--------------------------------|--------|
| CaCO ₃ | 95.088 |
| SiO ₂ | 1.112 |
| Na ₂ O | 0.354 |
| Al ₂ O ₃ | <0.01 |
| SO ₃ | 0.176 |
| MgO | 0.205 |
| Fe ₂ O ₃ | <0.005 |
| SrO | 0.116 |
| K ₂ O | <0.006 |
| P ₂ O ₅ | 0.087 |
| Cl | <0.009 |
| Br | 0.009 |
| ZnO | <0.004 |
| CuO | 0.01 |
| ZrO ₂ | 0.005 |

MS is generally made up of three layers, including an outer organic periostracum (made up of sclerotized proteins), a calcified prismatic layer, and an inner calcareous nacreous layer [16][17]. Calcite crystals, with diameters on the order of 2 μm and lengths of 50 μm ,

make up the outer prismatic layer [10]. These calcite crystals are allocated in a conchiolin matrix [10][18]. The inner layer, nacreous, consists of aragonite platelets enveloped in conchiolin (an insoluble protein) [17]. The platelets with a widths of 5–10 μm , for a single platelet, are highly ordered in parallel plates and with a small layer of an interlamellar organic matrix on top of each plate [10][19]. SEM of a *Mytilus edulis* shell in cross-section, in Figure 2 - 2, shows the morphologies and microstructure of MS [20].

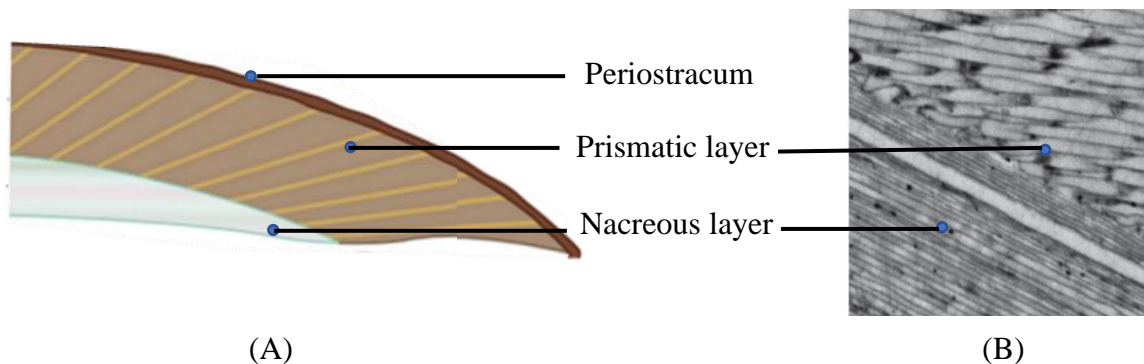


Figure 2 - 2: Section through the margin of shell of a *Mytilus edulis* (A) and SEM image of a *Mytilus edulis* shell in cross-section (B) [20]

The CaCO_3 in MS presents as two types of polymorphs: calcite and aragonite. These polymorphs have different dissolution rates, unit cell parameters, and space groups, so they would result in distinguishing powder XRD diffractograms [21]. The distribution of aragonite and calcite in MS is outlined in Figure 2 - 3 [21].

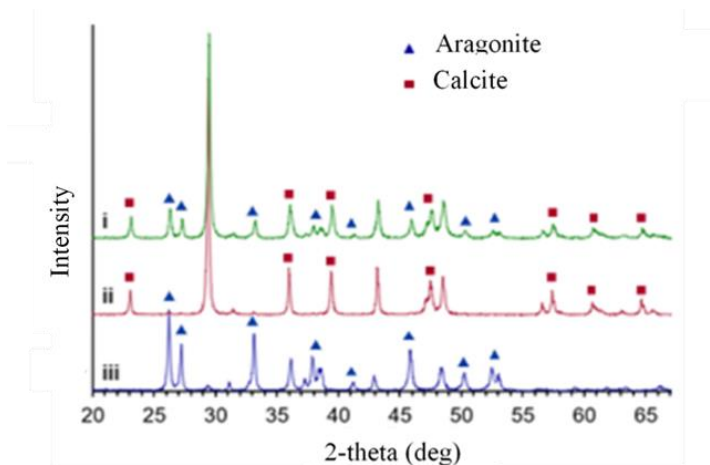


Figure 2 - 3: Powder XRD spectra for show the presence of calcite and aragonite in i) whole MS treated at 220 °C for 48 h, ii) outer, and iii) inner layers [21].

Fourier Transform Infrared spectroscopy (FT-IR) can identify the polymorphs as each polymorph has a unique IR spectrum [10]. Carbonate ions of CaCO_3 , CO_3^{2-} , have four fundamental modes of stretching: symmetric C-O stretch (ν_1 , 1083 cm^{-1}), CO_3^{2-} out of plane bending (ν_2 , 873 cm^{-1}), C-O asymmetric stretch (ν_3 , 1407 cm^{-1}), and O-C-O planar bending (ν_4 , 713 cm^{-1}). The ν_2 , ν_3 , and ν_4 modes indicate calcite (D_3 point group), and all four modes indicate aragonite (C_s point group) [10]. Aragonite can be distinguished by the positions of the ν_2 vibrations at 855 cm^{-1} or a pair of ν_4 peaks at 700 and 704 cm^{-1} [22]. While Gerhard et al., (2017) said that aragonite transformed to calcite heating at 300-400

°C, Murphy et al., (2019) showed calcite converts to aragonite if shells are heated to 220°C, Figure 2 - 4 [10][19].

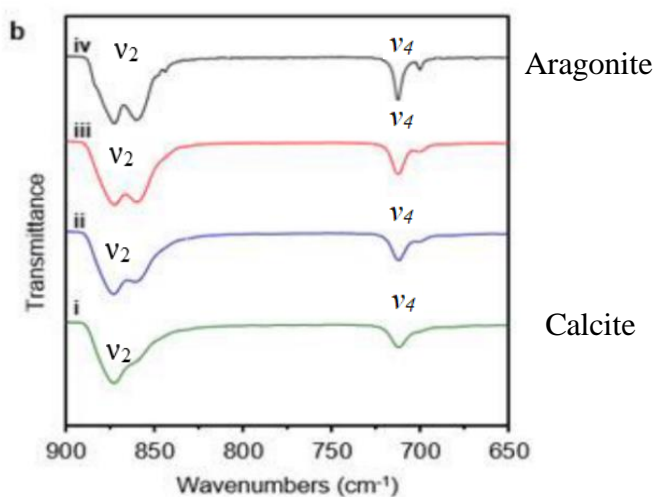
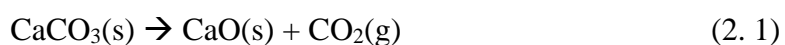


Figure 2 - 4: FT-IR spectra of (i) untreated blue mussel shells (ii) shells heated to 160 °C (iii) shells heated to 200 °C and iv) shells heated to 220 °C for 48 h [21]

CaCO₃ in MS can be converted to CaO via calcination process as following equation.



TGA can be used to calculate the amount of volatile compounds in MS during the calcination period [21]. The thermal decomposition of MS is mainly accounted for CaCO₃, which converts to CaO and CO₂ via calcination. The calcination process of MS initiates at approximately 650 °C in a nitrogen or oxygen environment [21]. The effect of calcination temperature on the conversion to CaO of CaCO₃ in MS is outlined in Figure 2 - 5.

As noted above, the residual meat in the WMS is a potential source of protein. The amino acid profile of mussel meat is outlined in Table 2- 2 [23].

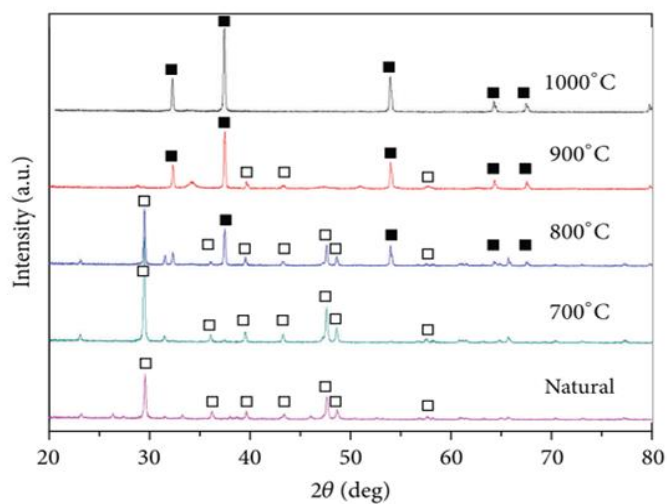


Figure 2 - 5: Powder XRD spectra of natural and CMS at different temperature

(□: CaCO₃, ■:CaO) [51]

Table 2- 2: Amino acid profile (g/100 g protein) of mussel meat [23]

| Compositions | g/kg |
|---------------|-------|
| Crude protein | 711 |
| Crude fat | 88 |
| Ash | 99 |
| Amino acids | |
| Alanine | 35.93 |
| Arginine | 53.24 |
| Aspartic acid | 73.14 |
| Cysteine | 11.06 |
| Phenylalanine | 26.41 |

| | |
|---------------|-------|
| Glutamic acid | 97.07 |
| Glycine | 40.43 |
| Histidine | 14.5 |
| Isoleucine | 32.76 |
| Leucine | 50.22 |
| Lysine | 53.45 |
| Methionine | 17.73 |
| Proline | 27.25 |
| Serine | 35.3 |
| Threonine | 33.13 |
| Tyrosine | 28.31 |
| Valine | 34.61 |

Conclusively, both the waste shells and the residual meat can be exploited as the added-value by-products. MS is a rich source of bio-CaCO₃ applied for industries. The hydrolysate of residual meat has potential applications for low-value by-products such as animal food or fishmeal [23].

2.3 Potential applications of waste mussel shells

WMS is a potential source of renewable CaCO₃, which can be utilized in several industries. Reviews of the applications of WMS are available in Morris et al. (2019); Naik and Hayes (2019); and Hart (2020).

2.3.1 Calcium supplement

MS can be directly used as a calcium supplement for livestock to improve bone health as well as the quality and strength of eggshells. MS contains up to 34.2 wt.% calcium, which could replace ground limestone as a calcium supplement in chicken feed, supplying calcium for bone and eggshell formation [25]. McLaughlan et al. (2014) investigated whole dried mussels as a supplement for poultry feed. Whole Zebra mussels were dried at 60 °C for 24 h prior to being finely ground (<2 mm). The finely ground mussel powder was added to the standard feed at two levels, 7.5 and 15 wt.%. The diet supplemented by mussel powder was used to feed 16-week-old Hy-Line brown chickens for six weeks. The results indicated that whole ground mussel powder was a promising supplement for chickens as it supported eggshell formation [26].

2.3.2 Soil amendment

MS can be used directly or indirectly as a calcium source to improve specific properties of soils. There are a number of studies on using MS as a soil amendment and its optimum dose for different purposes. Álvarez et al., 2012 investigated ground MS as a soil amendment and compared its performance to commercial lime derived from limestone in improving soil cation exchange capacity and aluminum (Al) saturation [27]. The study was carried out on four different types of ground MS, including coarsely ground dried MS (2-4 mm), finely ground dried MS (0-2 mm), coarsely ground calcined MS (0-2 mm) (CMS), and finely ground CMS (<63µm). All four MS-amended soils showed an increase in pH and exchangeable Ca, and a decrease in exchangeable Al and Al saturation [27]. Finely

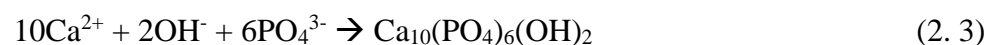
ground CMS (calcined at 550°C) showed the “best” performance, similar to those of using the commercial lime [27]. MS has been used to enhance the capacity of mine-impacted soils in adsorbing heavy metals (Cd, Cu, Ni, Pb, and Zn) to reduce migration of these metals to watersheds (Garrido-Rodriguez et al., 2014; Fernández-Calviño et al., 2016; Núñez-Delgado et al., 2017). Garrido-Rodriguez et al., (2014) studied the adsorption and desorption of Cd, Cu, Ni and Zn in a mine soil amended by MS ground to a particle size less than 1 mm. The adsorption capacity was a function of the initial concentration of the metals, while desorption was a function of both the concentration of metal and the dose of ground MS. As the MS dosage increased from 6 to 24 g kg⁻¹ the retention of Cd, Cu, Ni and Zn increased, with almost 100% mass retention for all 4 metals in 32 h for 24 g kg⁻¹ MS. Fernández-Calviño et al., (2016) used ground MS (<1mm) to treat Cu mining impacted soil and studied the changes in Cd, Cu, Ni, Pb and Zn retention of soil. Two different application doses of ground MS were investigated (12 and 48 Mg ha⁻¹). MS amendment at higher doses enhanced the retention in soil. Núñez-Delgado et al., (2017) compared Cd and Pb sorption/desorption of soil amended by finely ground MS, oak ash, pine bark, or hemp waste at 48 t ha⁻¹. Finely ground MS and oak ash showed the highest sorption (>99%) and the lowest desorption (<0.26%). Quintáns-Fondo et al., (2016) investigated finely ground MS (<1mm) as a bio-amendment to treat fluoride pollution in soils. The experiments used four different types of material: forest soil, a vineyard soil, pyritic material, and granitic material. All were treated with 48 t ha⁻¹ ground MS. MS-based amendment increased the fluoride sorption and decreased desorption. MS amended pyritic material showed the highest sorption (up to 90%) and the lowest desorption (10%). Osorio-López et al., (2014) studied ground MS (<1mm) for As (V) adsorption and desorption

capacity in forest and vineyard soils. The soil samples were amended with 24 t ha^{-1} ground MS. MS-amended soils increased the adsorption and decreased the desorption on As(V) relative to non-amended soils. Seco-Reigosa et al., (2015) also studied As(V), as $(\text{Na}_2\text{HAsO}_4 \cdot 7\text{H}_2\text{O})$, adsorption/desorption capacity using granitic material amended with finely ground MS ($<1 \text{ mm}$) at 12 and 24 t ha^{-1} . The finely ground MS amendment enhanced As(V) adsorption capacity of granitic material (99%) at pH near 8 [33].

2.3.3 Wastewater treatment

Commercial lime, CaO, is commonly used in wastewater treatment. MS, with the high levels of CaCO_3 , could serve as a surrogate for the lime. Jones et al. (2011b) studied CMS in phosphate removal from wastewater. The calcination process parameters were varied to determine the impact of degree of calcination. Calcination temperature was varied from $600\text{--}800 \text{ }^\circ\text{C}$, heating rate from $5\text{--}20 \text{ K min}^{-1}$, hold time over $1\text{--}5 \text{ h}$, and nitrogen flow of $0.5\text{--}2.0 \text{ L min}^{-1}$. The CaO formation increased with temperature. The conversion of CaCO_3 to CaO increased with particle size decrease, and at any temperature, the highest conversion was for particles ranging from 106 to $150 \text{ }\mu\text{m}$. However, for very small particle sizes, ground CMS would "sinter" together, decreasing the surface area. Slower heating rates and higher flow rates of nitrogen resulted in higher conversion to CaO. Conversion increased with the holding time of calcination. The maximum conversion (95%) occurred at $800 \text{ }^\circ\text{C}$, 5 K min^{-1} , 0.5 L min^{-1} nitrogen, and 3 h . Batch experiments were then carried out to determine the potential of raw and ground CMS in phosphate removal. The results showed that both finely ($53\text{--}106 \text{ }\mu\text{m}$) and coarsely ($212\text{--}250 \text{ }\mu\text{m}$) ground MS could remove approximately 20–30% of the phosphate, while the finer size range was more effective.

Both coarsely and finely ground CMS resulted in over 90% removal of phosphates within the first 5 min of the experiments. Adsorption on the surface of the particles was proposed as the only mechanism of ground MS, while precipitation was considered as the dominant mechanism for the ground CMS as outlined in reaction (2) and (3) [34].



Ji et al. (2019) studied modified CMS powder (average 75 μm) as a support to immobilize microalgae (*Chlorella*-sp) by adsorption via electrostatic interactions for phosphorous removal from contaminated water. MS was calcined at 700 $^\circ\text{C}$ for 2 h under vacuum. The CMS powder was activated by K_2CO_3 (K-CMS) via a hydrothermal process at 160 $^\circ\text{C}$ for 24 h to enhance the degree of dispersion of K and pore diameter [35]. The Zeta potential of *Chlorella*-sp and K-CMS were negative at pH 7, and therefore the K-CMS was modified with L-ARG to alter the surface to positive charge at pH 7. The K-CMS powder modified with L-ARG increased the effectiveness of the immobilization of *Chlorella*-sp. The final powder removed 95.0% of N and 88.63% of phosphorous at 25 $^\circ\text{C}$ [35].

MS has been studied as wastewater treatment process for the textile and dye industry. El Haddad et al. (2014) investigated CMS as bio-sorbent to remove textile dyes (Rhodamine B, Alizarin Red S, and Orange II) from aqueous solutions. MS was crushed and calcined at 900 $^\circ\text{C}$ over 2 h. The residue was then ground into small particles of 100-250 μm and

calcined at a heating rate of $2\text{ }^{\circ}\text{C min}^{-1}$ to $400\text{ }^{\circ}\text{C}$ and maintained at this temperature for 4 h. The dye removal was studied as a function of solution pH, CMS dose, dye concentration, temperature, and contact time. The optimum pH for Rhodamine B sorption was 9, and between 4 to 6 for Alizarin Red S and Orange II. The adsorption increased with the increase of CMS amount and the contact time (up to 60 min). The maximum biosorption capacity was 45.67 mg g^{-1} for Rhodamine B, 39.65 mg g^{-1} for Alizarin Red S, and 41.75 mg g^{-1} for Orange II [36]. Papadimitriou et al. (2017) used ground MS with several sizes (63, 125, 250, 350, and $500\text{ }\mu\text{m}$) for the removal of dyes (methyl blue and methyl red) and heavy metals (Cr (VI) as $\text{K}_2\text{Cr}_2\text{O}_7$, Cd as CdSO_4 and Cu as $\text{CuSO}_4\cdot 5\text{H}_2\text{O}$) from aqueous solutions. Ground MS at the smallest size ($63\mu\text{m}$) achieved near 100% methyl blue and methyl red removal from prepared dye wastewater in 14 days [37]. The removal of Cr(VI) and Cd (~100 %), was higher than the removal of Cu [37]. Ennil Bektaş (2017) investigated ground MS and other natural based materials (limestone, pumice, sepiolite, bentonite) as flocculant for a coagulation-flocculation process at paint and construction chemicals wastewater treatment plant. The pH, color, and electrical conductivity of treated wastewater were analyzed. Treated wastewater had a pH value in the range of 5–7, color value (Pt-Co) of 6 (similar to those of pure water clarity), and a low electrical conductivity of 1.1 mS cm^{-1} . Using the MS decreased the plants operating costs by approximately 90% [38].

Dandil et al. (2019) prepared CaO from MS for crystal violet, a triphenylmethane dye, removal from waste effluents of textile dyeing and paper printing industries. Crush MS were calcined at $900\text{ }^{\circ}\text{C}$ over 2 h at a heating rate of $5\text{ }^{\circ}\text{C min}^{-1}$. Treated MS were then further treated at $400\text{ }^{\circ}\text{C}$ over 2 h at a heating rate of $2\text{ }^{\circ}\text{C min}^{-1}$. The adsorption capacities

of the ground CMS (2 μm) for crystal violet in aqueous solution were investigated as a function of pH, adsorbent dosage, contact time, initial dye concentration, and temperature. The highest crystal violet adsorption of 482.0 mg g^{-1} was at pH 6, 0.2 g L^{-1} adsorbent dosage, 220 min contact time, and 25 $^{\circ}\text{C}$ for an initial dye concentration of 100 mg L^{-1} [39].

Photocatalytic degradation is a potential method to eliminate soluble organic dyes from aqueous solutions [40]. MS has been studied as support for photocatalyst, due to high surface area and chemical stability (Cai et al., 2019; McCauley et al., 2009). Echabbi et al. (2019) synthesized a heterogeneous photo-catalyst using CMS doped with titanium (Ti_2O) for the photo-degradation of methylene blue dye. Crushed MS was calcined at 900 $^{\circ}\text{C}$ for 2 h, and further dried at 80 $^{\circ}\text{C}$ for 24 h prior to being finely ground in small particles of 100-200 μm . The MS powder was then post-calcined at a rate of 2 $^{\circ}\text{C min}^{-1}$ to 400 $^{\circ}\text{C}$ and maintained at that temperature for 4 h. The obtained CMS powder was mixed with of TiO_2 at different ratios (using a minimum amount of water) and heated at 100 $^{\circ}\text{C}$ for 12 h. The obtained-dried material was ground to obtain a homogeneous mixture prior to the final calcination at 400 $^{\circ}\text{C}$ for 4 h. Photo-degradation of methyl blue was carried out to determine the capacity of the prepared catalyst of CMS/(10%-50%) TiO_2 [40]. Higher percentage of TiO_2 resulted in higher rates of degradation of methyl blue. A 60% MS powder and 40% TiO_2 mixture showed the highest discoloration yield at 80%; however, the rate of degradation did not increase as TiO_2 was increased to 50% [40]. Cai et al., (2019) studied MS as catalytic support for Bi_2MoO_6 . The $\text{Bi}_2\text{MoO}_6/\text{CMS}$ photocatalyst was then used to remove Rhodamine B dye in an aqueous solution under visible-light ($\lambda > 420 \text{ nm}$) irradiation. MS was calcined at 900 $^{\circ}\text{C}$ for 3 h at a heating rate of 10 $^{\circ}\text{C min}^{-1}$ and a nitrogen

flow of 100 mL min⁻¹. Bi(NO₃)₃·5H₂O, Na₂MoO₄·2H₂O was used to synthesize the Bi₂MoO₆/CMS photocatalyst (mass ratio of 7:4). Rhodamine B was degraded by 11% by CMS, 69.2% by pure Bi₂MoO₆, and 94.4% by Bi₂MoO₆/CMS [41].

MS has also been used to treat acid mine drainage (AMD) in passive bioreactors. Traditionally in these bioreactors, an alkalinity generating material (usually limestone) and a mixture of organic materials (compost, wood chips, manure, etc.) are prepared as a substrate for bacterial growth [43]. The bacteria, typically sulfate-reducing bacteria and other decomposer microorganisms, convert the sulfate in the AMD into hydrogen sulfide and neutralize the low pH through the bicarbonate. The hydrogen sulfide reacts with the dissolved metals in AMD and precipitates as insoluble metal sulfides and hydroxy-sulfates [43]. McCauley et al. (2009) studied MS to remove metals (mainly Fe and Al) and sulfate from AMD in a passive bioreactor. MS was used as the alkaline generating source and mixed with organic carbon materials (bark, post-peel, and compost) then added to the bioreactor. The mixture of MS was more effective for metals and sulfate treatment compared to mixtures of limestone [42]. Uster et al., (2014) investigated MS to treat AMD (pH<3, Fe>100 mg/L, and Al>40 mg/L), in a passive bioreactor system. In the first trial, MS replaced limestone in a mixture with organic materials (compost, wood chips, manure). MS performed better than limestone in alkalinity generation. In a second trial, MS was used as a single substrate material, as the MS provides not only a source of alkalinity but also the organic matter and a solid matrix. The results indicated the MS was effective as a single substrate. [43].

2.3.4 Filler

In addition to wastewater treatment, MS powder has been studied as a natural filler in the plastic industry. Yerlesen (2016) prepared a low-density polyethylene (LDPE)-based composite using mussel-oyster shell powder as a natural filler at 5, 10, and 15 wt.% shell powder. The shells were washed, dried, ground, and sieved to less than 50 μm . Increasing mussel/oyster shells wt% resulted in an increase in hardness, elasticity modulus, Izod impact strength, and density; and decrease of ductility and elongation of the LDPE-based composite [44]. Hamester et al. (2012) investigated CMS as a bio-filler in polypropylene (PP). The MS was heated in an oven at 200°C for 1 hour. The more brittle shells were milled in a high-speed planetary mill for 15 min with water, and the powders heated again to 500°C for 2 h. The powder was then re-milled to separate clusters. The CMS-derived filler contained 95.7 wt.% of CaO, lower than the commercial CaCO₃ (99.1 wt.%) filler. The CMS powder had a broader particle size distribution compared to commercial CaCO₃. Compared to PP/commercial CaCO₃, the PP/CMS composites showed similar thermal stability, melting temperature, and percent of crystallinity, higher temperature of onset decomposition (dO), and a maximum of decomposition (doff); and lower oxidation induction time. The mechanical properties were not significantly different in terms of Young's modulus, yield strength, and impact strength between PP/commercial CaCO₃ and PP/CMS. However, the elongation of the break of PP/CMS (26%) was lower than PP/commercial CaCO₃ (61%), which could be due to particle size distribution differences [45]. The structure, thermal and mechanical properties of the final plastic composites were determined as a function of the filler content, filler particle size, and processing conditions. Koçhan (2019) investigated the mechanical properties of WMS-based filler reinforced epoxy composites. The MS-based reinforced epoxy composites were prepared with a mix

ratio of resin to ground MS of 25:8 by mass. The produced MS-based reinforced epoxy composites had a micro-hardness level of 170 HV (the Vickers Pyramid Number), a tensile strength of 24 MPa, a compression strength of 11.28 MPa, and 75 MPa flexural strength [46].

2.3.5 Construction

Sand and gravel are key ingredients in cement, mortar, plaster, *concrete*, and blocks. Waste shells have properties that could supplement/replace sand and gravel in construction materials. Periwinkle shells are the most common mollusk's shells used in concrete, followed by the oyster, scallop, and MS [47]. Different particle size distributions and amount of fine and coarse MS in concrete were studied to determine the optimum ratio of shells to traditional sand and gravel (Martínez-García et al., 2019; Martínez-García et al., 2017; Rezaei et al., 2013). Martínez-García et al. (2019) investigated changes in properties of air lime coating mortar when MS sand was used as aggregate to replace limestone sand. Two different air limes were used as binders; a non-aged hydrated commercial lime powder and a 10-month slaked lime putty. MS was heated at 135 °C for 3 h then crushed to 4 mm and 1 mm powder. Powdered MS were mixed to obtain mussel sand that had a similar particle size distribution to the limestone sand and a fineness modulus of 3.71. The limestone aggregate was replaced with MS sand at 25, 50, and 75 wt.%. The higher percentages of MS-derived aggregate presented problems in properties of the MS-based mortar, such as lower consistency, irregular pore size distribution (due to the organic matter content), strength reduction, and higher carbonation degree [15]. Substitution at 25 wt.% produced a lime-based mortar having suitable characteristics for use as a base-layer coating

and as a surface-layer coating [15]. Peceño et al. (2019) studied the substitution of coarse aggregates with CMS in acoustic-absorbing concrete. The cleaned MS was dried at 190°C for 18 min prior to being crushed and then calcined at 500 °C for 1 h. The CMS-based (2-7mm) acoustic-absorbing concrete resulted in a 40% increase in the weighted acoustic absorption coefficient compared to the traditional river grave concrete. The mechanical properties analysis of CMS-based concrete was superior in all specimens over the traditional concrete, especially in compression strength [50]. Martínez-García et al. (2017) evaluated MS as an aggregate in plain concrete. MS were treated at 135 °C for 32 min, then ground to three different particle sizes: 0–4 mm (natural sand), 4–16mm (fine MS aggregates), and 10–20 mm (coarse MS aggregates). Treated MS was varied from 5, 12.5, 25, 50, 75, and 100 wt.%. In general, the CMS replacement should be limited to 25 wt.% of fine or coarse aggregates or 12.5 wt.% for both fine and coarse aggregates [48]. Greater than 25 wt.% CMS aggregates reduced mechanical properties (strength and modulus), water absorption, and water permeability of the concrete. The organic fraction of the MS (residual organic compounds and organic matrix of the shells) increased porosity, setting time and paste viscosity and decreased the aggregate-paste bond, the liquidity of the mix, and mechanical performance of the concrete [48]. This highlights the benefit of removing the residual organics.

2.3.6 Catalyst

High purity CaO derived from WMS can be used as a catalyst in transesterification to produce biodiesel. Buasri et al. (2013) investigated mussel, cockle, and scallop shells as catalysts for the transesterification of palm oil to biodiesel. The dried waste shells were

calcined at 1000 °C in an air atmosphere at a heating rate of 10°C min⁻¹ for 4 h. The obtained shells were ground to size 38–75 µm. Calcined cockle shells had the highest concentration of CaO (99.17 wt.%) followed by MS (98.37 wt.%), while CMS showed the highest surface area (89.91 m²/g), pore volume (0.130 cm³/g), and mean pore diameter (34.55 Å). The reaction time, temperature, methanol:oil ratio, and catalyst loading were varied to investigate the yield of biodiesel. The highest conversion (95%) obtained for all calcined shells was at 65 °C, molar methanol:oil ratio of 9:1, catalyst loading 10 wt.%, and reaction time of 3 h [51]. The study indicated that CMS, as well as other calcined shells are promising alternatives for cost-effective and environmental-friendly catalysts for biodiesel production [51]. Rezaei et al. (2013) investigated the optimization of biodiesel production of soybean oil using a WMS-based catalyst. Ground MS (125-250 µm) was calcined at 950, 1000, and 1050 °C for 2 h. For each type of MS-based catalyst, the transesterification reaction was conducted at different catalyst concentrations (6, 9, and 12 wt.%) and molar ratios of methanol:oil (12:1, 18:1, and 24:1) at 60 °C for 8 h. The maximum biodiesel production occurred using a 12wt% MS-based catalyst (produced at 1050 °C) and the ratio of methanol:oil of 24:1. The maximum yield was 94.1%, with 100% purity [49]. Mohadesi et al. (2018) investigated the effects of stirrer speed (250 and 350 rpm), reaction temperature (55, 60, and 65 °C), and reaction time (1, 3, 5, 7, and 8h) on the transesterification of soybean oil using 12wt% MS-based catalyst (produced at 1050 °C).

2.3.7 Hydroxyapatite production

Hydroxyapatite (HA, Ca₁₀(PO₄)₆(OH)₂) is an essential component of bone and teeth [53]. The dominant application of HA is a bone filler and a coating material for implants [53].

HA is typically produced from corals via two main processes; hydrothermal and wet chemical precipitation [54]. Jones et al. (2011a) proposed a simple wet chemical process for the formation of HA from WMS. The crushed MS were calcined at 800 °C in a nitrogen environment. The conversion of CaCO_3 to CaO was greater than 95% for all sizes. Crushed CMS was mixed with deionized water to produce a suspension of calcium hydroxide ($\text{Ca}(\text{OH})_2$) and mixed with monopotassium phosphate (KH_2PO_4) solution to form precipitation of HA. The HA contained impurities and had poor crystallinity compared to the commercial HA. However, the post-washing and heating processing removed the potassium impurity and improved the crystallinity of MS-based HA. The final MS-based HA showed similar quality with commercial HA. The biocompatibility of MS-based HA was also studied, and the MS-based HA stimulated cell growth and promoted mineralization [53]. Ramli et al. (2012) prepared HA-nanoparticles biomaterials from MS by wet precipitation assisted with microwave irradiation. Coarsely crushed MS were treated with hydrochloric acid to remove organics and calcined at 900 °C over 2 h. The CaO was converted into $\text{Ca}(\text{OH})_2$ by adding H_2O . The pH was maintained at 9 using NH_4OH . Di-ammonium hydrogen phosphate [DAP, $(\text{NH}_4)_2\text{HPO}_4$] solution was added to the $\text{Ca}(\text{OH})_2$ suspension and irradiated using microwave 30, 45, 60, 75, 90, and 120 min. The produced HA was filtered, oven-dried, and powdered. The obtained HA powders were nano size, which increased from 10 nm at 30 min to 55 nm at 120 min of irradiation. $\text{Ca}(\text{OH})_2$ is considered an impurity in the final nano HA, the content decreased with an increase of the irradiation time, and almost disappeared at 120 min [54]. Shavandi et al. (2015) proposed a rapid microwave irradiation method to prepare nano-crystalline HA from MS using ethylenediaminetetraacetic acid (EDTA). MS was first dried overnight at

80 °C, then calcined at 900 °C for 30 min. The obtained CMS was finely ground. The solution of Ca-EDTA complex was mixed with disodium hydrogen phosphate (Na_2HPO_4). The pH was maintained at 13. The mixture was heated in a microwave at 1100W until dried. The obtained precipitated HA was washed to remove residual Na and EDTA and dried in a vacuum oven at 80 °C for 6 h. The crystal phase composition, functional groups, thermal stability, microscopic details of the surface, crystal size, and morphology were determined. The HA product showed competitive properties (phase purity, crystal size and shape, thermal stability, and porosity) to a commercial HA [55]. Kumar et al. (2017) developed a single step, simple, and rapid method to synthesize HA from MS by using microwave irradiation and EDTA. The cleaned MS were dried at 110 °C for 5 h in a hot air oven prior to being crushed into powder and mixed with EDTA, and then Na_2HPO_4 solution was added. The pH was maintained at 13 by using NaOH. The mixture was subjected to microwave irradiation at 700W power for 15 min. The precipitated HA was washed with distilled water and dried in the hot air oven at 110 °C for 5 h. The synthesized HA powder was a B-type carbonate substituted HA having flower-like morphology, which could be used as a biomaterial for orthopedic applications [56]. Sari and Yusuf (2018) used the precipitation method to synthesize HA for implant applications from green MS. The finely crushed MS were calcined in a furnace at a temperature of 950 °C for 2 h, and $(\text{NH}_4)_2\text{HPO}_4$ solution was added. The liquid mixture was stirred (at 300 rpm) for 15, 30, and 45 min at 70 °C. The pH of the mixture was at 9 or greater by adding ammonium hydroxide (NH_4OH) (25%). The precipitated-filtered HA was dried at a temperature of 100 °C for 2 h. The post calcination of HA was carried out at 950 °C for 3 h in a furnace to produce the pure HA. The synthesized HA under the stirring time of 15 min showed higher

stability and transmittance value compared to longer stirring times. The crystallization of HA depended on the stirring time, and no more HA was formed as the stirring time was longer than 15 min. HA, with the stirring time of 15 min, also had a small agglomerate shape and thick structures of particles [57].

MS-derived HA has been utilized in wastewater treatment. Meski et al. (2019) synthesized HA powder from MS, using a wet precipitation process, for Cd (II) removal from aqueous solutions. The ground MS was calcined at 900 °C for 30 min, and $\text{NH}_4\text{H}_2\text{PO}_4$ is added to react with calcined ground MS at room temperature without pH control. The produced HA was dried at 80 °C for 24 h to obtain the final product. The mussel-derived HA was then used in Cd as $(\text{Cd}(\text{NO}_3)_2 \cdot 4\text{H}_2\text{O})$ adsorption from aqueous solutions. The adsorption followed a two-step mechanism with a rapid ion exchange with Ca^{2+} followed by the dissolution of HA and the precipitation of the CdHA. The adsorption process was endothermic with a Langmuir isotherm with a maximum adsorption at 60 min [58]. El-Bassyouni et al. (2019) synthesized HA nanoparticles from MS using a wet chemical precipitation process. The synthesized HA was then used to remove cesium-137 (^{137}Cs) and europium-152+154 ($^{152+154}\text{Eu}$) from radioactive liquid wastes. CaCO_3 in MS powder was converted to $\text{Ca}(\text{NO}_3)_2$ by reacting with HNO_3 and mixed with $\text{NH}_4\text{H}_2\text{PO}_4$ to form HA at a pH of 9. The precipitated HA was dehydrated in a dryer at 70 °C for three days prior to crushing, and the powder was finally calcined in an oven at 900°C. The adsorption capacity of the prepared HA for ^{137}Cs and $^{152+154}\text{Eu}$ was tested as a function of pH (2-12), sorbent dose (0.025 – 0.25 mg), and contact time (5 – 210 min). The pH value had a greater impact on $^{152+154}\text{Eu}$ removal than ^{137}Cs removal. The removal of ^{137}Cs increased 28 to 50%

as the pH value changed from 2 to 7 then maintained, while the $^{152+154}\text{Eu}$ was increased from 52 to 99% as the pH increased from 2 to 12. The increase of sorbent dose and contacting time led to the increase of the removal for both metals, but was more significant for $^{152+154}\text{Eu}$ than ^{137}Cs [59]. The maximum removal under optimum condition was up to 99 wt.% for both ^{137}Cs and $^{152+154}\text{Eu}$ [59]. Shariffuddin et al. (2013) synthesized HA from MS using a pyrolysis–wet slurry precipitation process. The received HA was then used as a photocatalyst for wastewater remediation. MS was calcined at 800 °C for 5 h under nitrogen flow to convert CaCO_3 to CaO . HA was precipitated using potassium dihydrogen phosphate (KH_2PO_4), and the precipitated HA was separated from the solution and dried in an oven at 110 °C overnight. Methylene blue was degraded using the MS-derived HA as a photocatalyst under both oxygen-limited and oxygen-rich conditions. The oxygen-rich conditions led to a greater decolorization (62% after 24 h) compared to the oxygen-limited condition (39% after 6 h) [60].

As shown above, MS is a valuable source of bio- CaCO_3 , and could serve as an alternative to commercial CaCO_3 . However, the bulk of the research is at lab-scale and on meat-free MS, while in industry, WMS is discarded with a certain mass of residual meat. The residual protein of WMS causes difficulties for the treatment of waste and hinders the utilization of WMS as a source of renewable CaCO_3 . The decomposition of the residual protein of WMS significantly impacts on the storage of WMS and the purity of the produced bio- CaCO_3 or CaO . Overall, it is a significant challenge that the mussel processing industry must deal with to approach sustainable development.

2.4 Protein enzymatic hydrolysis in by-products of fish processing

Enzymatic hydrolysis is a process used to enhance value and diversify the types of products from food processing [61]. Enzymatic hydrolysis has been used to hydrolyze fish protein for applications in food modifiers (water-holding, emulsification, solubility, oil binding capacity, and texture properties) [62] and production of bioactive peptides (Karnjanapratum and Benjakul, 2017; Sinthusamran et al., 2019) among others. By-products of fish processing are rich sources of proteins [65].

Sinthusamran et al., (2019) utilized Pacific white shrimp (*Cephalothorax*) processing by-products to produce shrimp protein hydrolysate for biscuit fortifier using Alcalase from *Bacillus licheniformis*. The amount of added shrimp hydrolysate-based fortifier impacted properties of the biscuit such as shape, hardness, fractur ability, surface, and color. Adding 5 wt.% of shrimp hydrolysate-based fortifier increased the protein content and decreased the carbohydrate content in the biscuit. Volatile compounds (aldehyde, ketone, alkane and ether) in the shrimp hydrolysate-based fortifier contributed to odor and flavor of the resulting biscuit [64]. Zhou et al., (2016) evaluated dry hydrolysate from squid processing waste (heads, viscera, skin, fins, and small tubes) and scallop viscera (the remainder after collecting adductor muscle) as specialty ingredients in plant-based (soybean, corn, and whole wheat) diets of Pacific white shrimp *Litopenaeus vannamei*. Squid and scallop hydrolysate were determined to be nutrient sources and could be incorporated in the shrimp feed formulations to enhance nutritional value [66]. Novriadi et al., (2017) produced dried squid hydrolysate from squid processing by-products (heads, viscera, cut-offs, fins, and small tubes) and investigated as a supplement in plant-based fishmeal for

Florida pompano (*Trachinotus carolinus*) feed. Squid hydrolysate containing high protein levels (72.19 wt. %) and a moderate level of lipid (9.03 wt.%) were added at 1, 2, and 4 wt.% to the plant-based diet for pompano over 56 d. The diet with 4% squid hydrolysate showed better nutritional value and increased the percentage of higher quality fish product [67]. By-products of fish processing industry have been an attractive source of protein.

In the mussel processing industry, enzymatic hydrolysis has been used to produce food ingredients, supplements, stabilizers in beverages, natural flavors, antimicrobial agents, and a cardio-protective nutrient [68]. Normah (2018) evaluated umami taste, one of the five basic tastes that contribute to palatability and savory taste in food, of protein hydrolysates derived from green mussel (*Perna viridis*) using a flavoenzyme. Amino acids which contribute to umami taste include glutamic acid, glycine, and aspartic acid. The mussel hydrolysates showed protein size range between 10 to 70 kDa and contained the amino acids that contribute to umami taste. In the context of sensory evaluation, mussel hydrolysate did not have the strong odor and flavor associated with fish, so it could be used as a natural flavor [69]. Silva et al., (2010) investigated hydrolysis of mussel meat by using Protamex, a mixture of serine and metalloendopeptidas obtained from *Bacillus licheniformis* and *Bacillus amyloliquefaciens*. Degree of hydrolysis (DH) is defined as the ratio of the number of peptide bonds cleaved (h) to the total number of bonds available for proteolytic hydrolysis (h_t). The degree of enzymatic hydrolysis (DH) was studied as a function of enzyme:substrate ratio and pH, and a model developed:

$$DH(\%) = 17.6 + 5.07 \cdot \frac{E}{S} - 2.07 \cdot pH + 1.57pH^2 \quad (2.4)$$

At pH 6.85, temperature 51 °C, and enzyme:substrate ratio of 9:2, the DH was 26.5%. The protein recovery (PR), defined as the ratio between the protein in the hydrolysate and the initial protein in the original substrate, was calculated as a function of enzyme:substrate ratio and pH. The following model was developed:

$$PR(\%) = 55.53 + 9.23 \cdot \frac{E}{S} - 1.32 \left(\frac{E}{S}\right)^2 + 1.22pH + 1.44pH^2 \quad (2.5)$$

The maximum PR was 65%. The hydrolysate had a lower fat content compared to the raw material. The mussel protein hydrolysate showed the same amino acid profile/composition as mussel meat (predominantly glutamic acid, aspartic acid and tryptophan). Protein bands identified included light myosin chains 1 and 3 (25 and 15 kDa) and peptides of molecular weight lower than 6.5 kDa [68]. The obtained mussel hydrolysate with a good nutritional value was suitable to produce a flavoring agent [68].

Xu et al., (2019) determined the osteogenic activity of *Mytilus edulis* protein. Fresh blue mussels (*Mytilus edulis*) were hydrolyzed using pepsin for 2 h followed by trypsin for 3 h. The water-soluble protein hydrolysate was isolated and analyzed for osteogenic activity. The protein hydrolysate had bioactive functions which would be beneficial for bone growth and health [70]. Dong et al., (2017) studied antioxidant activities of peptide fractions derived from freshwater mussel protein. Mussel protein hydrolysates were

prepared using ultrasound-assisted enzymatic hydrolysis with Neutrase 0.8 L. The antioxidation activity was the highest for the protein fraction less than 3 kDa [71]. Kim et al., (2012) prepared anticancer peptide from *Mytilus cooscou* via enzymatic hydrolysis using eight proteases including; papain, pepsin, α -chymotrypsin, and trypsin Flavourzyme, Neutrase, Protamex, and Alcalase. The hydrolysate obtained from pepsin hydrolysis consisted of Alanine, Phenylalanine, Asparagine, Isoleucine, Histidine, Arginine, and Leucine and had the strongest cytotoxic activity on prostate, breast, and lung cancer cells [72]. Qiao et al., (2018) investigated the antithrombotic activity of peptides produced from *Mytilus Edulis* protein. Water-, salt- and acid-soluble mussel protein were extracted according to solubility. The protein fractions were hydrolyzed by using trypsin (5000 U/g) at 45 °C, pH 8.5 for 3 h. The obtained hydrolysates were analyzed to determine thrombin inhibitory activity. The antithrombotic activity of mussel hydrolysate was 40.17%, 85.74%, 82.00% at 5 mg/mL for water-, salt- and acid-soluble mussel protein fractions, respectively [73]. Beaulieu et al., (2013) determined the protein hydrolysates produced from *Mytilus Edulis* processing by-products (whole raw mussels) have anti-proliferative activities, which is the ability of a compound to stop the growth of cells. Enzymatic hydrolysis using Protamex was conducted with whole mussels to generate the target bioactive peptides. The hydrolysates fractions less than 50 kDa had the highest anti-proliferative activity [74].

Naik and Hayes (2019) studied residual proteins in WMS as a source of high molecular weight proteins, bioactive peptides, and low molecular weight proteins (enzymes). These protein hydrolysates can find application in food, cosmetics, packaging, dyes, marine

technology and so on [8]. Nagel et al. (2017) conducted feeding experiment to test the potential of blue mussel hydrolysate as a replacer for fishmeal protein in diets of turbot. Partially replacing fishmeal protein by mussel hydrolysate in diets of turbot was not successful in stimulate the feed intake of turbot, but showed the same impact on turbot growth compared to using commercial fishmeal protein [75]. This indicates the nutritional and functional properties of mussel hydrolysate were comparable to fishmeal protein. Blue mussel hydrolysate could be exploited in aquafeeds fish [75].

A review of the literature showed only three studies on WMS where both the residual proteins and bio-CaCO₃ were evaluated. In a patent by Frude (2008) meat attached on whole or crushed MS was digested by enzyme solutions of Alcalase (pH of 8-9), Pepsin (pH of 3-4), or Papain at a specific pH (appropriate to the enzyme). The reaction required up to 2 h at 40-75 °C. Poor digestion of meat was observed with the larger WMS particles, some meat, especially tendrils and adductor, were undigested. If the shells were too finely crushed (sand-like) these particles carried over into the hydrolysate, presenting separation and purity issues. The optimal conditions for reactions and operation were not discussed, and the process uses costly enzymes [76]. Control of pH is also an operational issue.

In work by Murphy et al., (2018), Protex 6L (6L) and Protex 7L (7L) (standard food-grade enzymes by DuPont) were used to hydrolyze raw and cooked WMS with residual meat. The whole raw mussels were estimated to contain 50 wt.% meat. Meat of whole raw mussels was remove using 1.0-2.0 $\mu\text{L}\cdot\text{g}^{-1}$ 6L in seawater or tap water at 55 °C for 4 h. Cooked mussel meat (12g) was 97.2% digested using 6.0 $\mu\text{L}\cdot\text{g}^{-1}$ 7L in seawater for 10 h at 25 °C. The proposed enzymatic hydrolysis process was environmental-friendly, cost-

effective, and safe process due to low enzyme loading, seawater as media, mild temperatures, and elimination of acids and bases to control pH. The generated protein hydrolysate was proposed as a potential nutritional source for fishmeal [77]. However, the intact shell halves used for experiments of this work are not the typical type of WMS in industry and the impact of “mussel age” on the enzymatic meat removal process was not studied.

In 2020, Naik et al. used Protamex® (the new name of Multifect enzyme) to hydrolyze meat leftover on mussel by-products (undersized mussels, mussels with broken shells, and barnacle-fouled mussels) with controlled temperatures and agitation, and enzyme:substrate ratio of 1:50 (w:v). The degree of hydrolysis (DH) was determined using the Adler-Nissen pH stat method. The authors analysed obtained hydrolysates for protein content, amino acid composition, lipid content, fatty acid methyl ester composition, ash, and techno-functional and bioactive activities [78]. All the obtained hydrolysate samples contained essential compounds which have an anti-inflammatory property. The by-product mussel hydrolysates contain up to 91% of peptides which are identified to have angiotensin-converting enzyme I and dipeptidyl peptidase IV inhibitory activities. Results demonstrated that hydrolysates of mussel by-products have potential for use as health-promoting ingredients [78]. However, there was not study of the rate of reaction or variation of key operating parameters such as enzyme to substrate concentrations.

2.5 Kinetic models of protein enzymatic hydrolysis in by-products of fish processing

Kinetic studies of protein enzymatic hydrolysis are used to develop a rate model to describe and predict the enzymatic hydrolysis process. The Michaelis-Menten equations have been used to predict the rate of enzymatic hydrolysis of proteins since 1913. Sampedro et al., (2019) studied the effect of lipids on enzymatic hydrolysis of red tilapia viscera (*Oreochromis Sp.*) using Alcalase 2.4 L, a serine endopeptidase that consists primarily of subtilisin Carlsberg produced via fermentation of *Bacillus licheniformis*. The protein hydrolysis reaction was monitored through degree of hydrolysis (DH in %) by the pH-stat method. The concentration of the lipid in raw materials was varied (1, 19 and 50 g/L) to determine degree of inhibition on enzymatic hydrolysis. The rate of hydrolysis decreased as lipids concentration increased. Lipid inhibition was modeled via a Michaelis-Menten model. In the context of Michaelis-Menten model, it was assumed that enzyme was not consumed or inactivated during the hydrolysis process. A mechanism was proposed as following:



Where k_1 (s^{-1}), k_{-1} (mM/s), k_2 (mM/s), k_3 (s^{-1}), k_{-3} ($g/L \cdot s^{-1}$) are rate constants, K_M (mM) is the Michaelis-Menten constant, and K_I (g/L) is the inhibition constant. The experimental data were fitted with competitive (equation 2.8), uncompetitive (equation 2.9), and mixed inhibition models (equation (2.100) to determine the type of inhibition, and the kinetic parameters.

$$v = \frac{v_m S_0}{S_0 + K_M \left(1 + \frac{I_0}{K_I}\right)} \quad (2.8)$$

$$v = \frac{v_m S_0}{S_0 \left(1 + \frac{I_0}{\alpha_f K_I}\right) + K_M \left(1 + \frac{I_0}{K_I}\right)} \quad (2.9)$$

$$v = \frac{v_m S_0}{S_0 \left(1 + \frac{I_0}{\alpha_f K_I}\right) + K_M} \quad (2.10)$$

Where v_m (mM/s) is the maximum reaction rate, S_0 (mM, g/L) is the initial concentrations of substrate, I_0 (g/L) is the initial concentrations of inhibitor, and factor α_f . Lineweaver-Burk graphs were used to identify the constant of inhibition. The results indicated that the lipids strongly competed with protein or a competitive inhibition mechanism, (2. 8). The obtained kinetic model fit the experimental date well, $R^2 = 0.9936$.

$$v = \frac{0.036S_0}{S_0 + 54.98 \left(1 + \frac{I_0}{2.359}\right)} \quad (2.11)$$

Kinetic models have been developed based on changes of substrate or production concentration. Novikov et al., (2018) studied the enzymatic hydrolysis of homogeneous-ground Atlantic cod by-product (heads, fins, bones, and muscle tissue) using hepatopancreatine. The proteolysis was evaluated on the degree of hydrolysis (DH, %). The DH is calculated from the total nitrogen value (N_T , %), the amino nitrogen value (N_0 ,

(%) of non-hydrolyzed proteins, and the amino nitrogen value (N_A , %) of the hydrolysate [80].

$$DH = \left(\frac{N_A - N_0}{N_T - N_0} \right) \times 100\% \quad (2.12)$$

The model was divided into three potential phases; one where the easily hydrolyzed substrate (S) was degraded, a second where the hydrolyzed substrate (C) was hydrolyzed, and a third autolysis step. A mechanism was proposed as following.



Where k_1 , k_2 , k_3 (L/g.s) are rate constants. Based on the accumulation of the hydrolysis product which is the accumulation of amino nitrogen in the hydrolysate, the following equation was developed to describe the hydrolysis process:

$$\frac{d}{dt}p(t) = k_1e(t)s(t) + k_2e(t)c(t) + k_3e(t)^2 \quad (2.16)$$

Where $p(t)$ (g/L) is the total concentration of all products at t , $e(t)$ (g/L) is a concentration of enzyme at t , $s(t)$ (g/L) is a concentration of more reactive substrate at t , and $c(t)$ (g/L) is concentration of a concentration of less reactive substrate at t , t is time (s). Simulation of autolysis and optimisation of the reaction rate constant were carried out using Maple 2017.1 (Waterloo Maple, Inc., Canada). Using the initial conditions $C_{E(t \rightarrow 0)} = C_{E0}$, $C_{S(t \rightarrow 0)} = C_{S0}$, $C_{C(t \rightarrow 0)} = C_{C0}$, and $C_{P(t \rightarrow 0)} = 0$ (in g/L), the obtained equation was:

$$p(t) = -S_0 \left(\frac{1}{E_0}\right)^{\frac{k_1}{k_3}} e^{-\frac{k_1 \ln\left(k_3 t + \frac{1}{E_0}\right)}{k_3}} - C_0 \left(\frac{1}{E_0}\right)^{\frac{k_2}{k_3}} e^{-\frac{k_2 \ln\left(k_3 t + \frac{1}{E_0}\right)}{k_3}} - \frac{1}{k_3 t + \frac{1}{E_0}} + C_0 + S_0 + E_0 + P_0 \quad (2.17)$$

Where S_0 (g/L), C_0 (g/L), E_0 (g/L), and P_0 (g/L) are the initial concentrations of the substrates, enzyme, and product. The equation fit the data well at all enzyme concentration, with a $R^2 > 0.98$.

Table 2- 3: Rate constants (k_1 , k_2 , and k_3) for the intermediate stages of the enzymatic hydrolysis of the protein-containing raw materials (recycled waste product of cod) calculated from the proposed kinetic model; correlation coefficient (R_2)

| | Concentration of enzyme, g/L | | | | |
|----------------------|------------------------------|-------|------|-------|-------|
| Rate constant, L/g.s | 0.025 | 0.038 | 0.05 | 0.076 | 0.088 |
| | | | | | |

| | | | | | |
|------------------|-------|-------|-------|-------|-------|
| $k_1 \cdot 10^2$ | 9.3 | 13.6 | 9.3 | 9 | 13 |
| $k_2 \cdot 10^3$ | 1.4 | 1.9 | 1.7 | 2.1 | 1.6 |
| $k_3 \cdot 10^2$ | 0.7 | 1.3 | 1.2 | 1.9 | 1.3 |
| R^2 | 0.992 | 0.988 | 0.986 | 0.989 | 0.989 |

Novikov et al., (2018) investigated enzymatic hydrolysis of Atlantic cod by-product using hepatopancreatine using first-order kinetics. This model assumes that hydrolysis is a first-order reaction and the enzyme is not consumed during the reaction [80].



The hydrolysis curves, which describe the accumulated of amino nitrogen in hydrolysate, were fitted with the equation.

$$C_A = C_{A\infty}(1 - e^{-kt}) \quad (2. 19)$$

Where $C_{A\infty}$ is the value of C_A (concentration of amino nitrogen in hydrolysate) for $t \rightarrow \infty$, k is the rate constant, and t is the reaction time. However, results showed equation **Error!** **Reference source not found.** could not describe the entire length of the hydrolysis period.

Tan et al., (2019) investigated the hydrolysis of by-products (mostly heads and bone frames) of channel catfish (*Ictalurus punctatus*) fillet processing using different enzymes including papain, ficin, bromelain, neutrase, alcalase, protamex, novo-proD and thermolysin. The DH (%) was determined using the trinitrobenzenesulfonic acid (TNBS) method reported by Adler-Nissen [81]. The kinetics of the protein enzymatic hydrolysis was modeled based on Peleg's model at various temperatures.

$$DH(t) = \frac{t}{K_1 + K_2 \cdot t} \quad (2. 20)$$

Where DH(t) (%) is the degree of hydrolysis at time (t), DH(0) (%) is the degree of hydrolysis at time t =0, K₁ is Peleg's rate constant and K₂ is Peleg's capacity constant. The hydrolysis results fit well with Peleg's model with high value of R², higher than 0.91 for all enzymes and different reaction conditions. The Ficin enzyme was the most efficient enzyme with a DH of 71% at 30 °C for 120 min, K₁ = 1.80, K₂ = 0.44, R² = 0.93 [81].

Qi and He (2006) investigated the protein hydrolysis and single-substrate hydrolysis, enzyme inactivation, substrate inhibition, or product inhibition [82]. An exponential equation was used to model the DH [82].

$$\frac{d(DH)}{d(t)} = a \cdot \text{EXP}[-b \cdot DH] \quad (2. 21)$$

Where parameters a and b have different expressions based on if the process has no inhibition, substrate inhibition, product inhibition, or both product and substrate inhibition, Table 2- 4.

Table 2- 4: Expression of kinetic parameters a and b for exponential equation

| Mechanism | a | b | |
|-------------------------------------|---|---|---------|
| No inhibition | $\frac{k_2 e_0}{s_0}$ | $\frac{k_3 K_m}{k_2}$ | (2. 22) |
| Substrate- inhibition | $\frac{k_2 K_S e_0}{s_0 K_S + s_0^2}$ | $\frac{k_3 K_m K_S}{k_2 (K_S + s_0)}$ | (2. 23) |
| Product-inhibition | $\frac{k_2 K_P e_0}{s_0 K_P + p K_m}$ | $\frac{k_3 K_m K_P s_0}{k_2 (s_0 K_P + p K_m)}$ | (2. 24) |
| Substrate and product-inhibition | $\frac{k_2 K_S K_P e_0}{s_0 K_S K_P + K_P s_0^2 + p K_S K_m}$ | $\frac{k_3 K_m K_S K_P s_0}{k_2 (s_0 K_S K_P + K_P s_0^2 + p K_S K_m)}$ | (2. 25) |

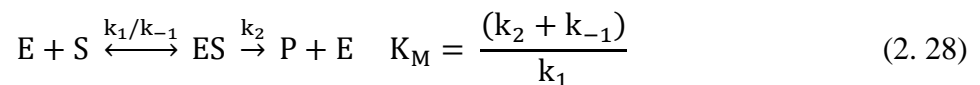
BSA-trypsin was selected as a model system, in which BSA is hydrolyzed by trypsin, to model the complex kinetic behaviour of enzymatic hydrolysis reaction [82]. Based on experimental results, a mechanism of substrate inhibition was proposed for the BSA-trypsin hydrolysis process. The final exponential kinetic equation was established, and the average relative error of the model is 4.73%.

$$\frac{d(DH)}{d(t)} = \frac{1147.5545e_0}{12.8598s_0 + s_0^2} \text{EXP} \left[-\frac{3.3677}{12.8598 + s_0} DH \right] \quad (2.26)$$

Based on the results in study of Qi and He (2006), Zapata Montoya et al., (2018) modeled protein enzymatic hydrolysis of viscera from red tilapia (*Oreochromis Sp.*) using commercial Alcalase 2.4 L, a non-specific bacterial endopeptidase from *Bacillus licheniformis* with Subtilisin Carlsberg. The hydrolysis process was observed via the DH (%) or as the ratio of peptide cleaved bonds (h) to the total peptide bonds in the raw material (h_t)

$$DH = \frac{V_b N_B}{M_p} \frac{1}{\alpha} \frac{1}{h_t} \times 100 \quad (2.27)$$

Where V_b is the volume of base consumed (L), N_B is the normality of the base (Eq-g/L), M_p is the mass of the protein (kg), and α is the average dissociation grade of the released groups $\alpha\text{-NH}_2$ in the reaction. DH was dependent on the initial concentration of substrate (S_0), enzyme (e_0) and the time (t). DH increased with an increase of initial enzyme loading and decreased with initial protein loading. The authors proposed a substrate inhibition mechanism for the hydrolysis.





Where k_1 , k_{-1} , k_2 , k_3 , k_{-3} are rate constants, K_M (mM) Michaelis-Menten constant, and K_S (g/L) the dissociation constant of SES. An kinetic model was developed from a standard exponential kinetic equation.

$$\frac{d(DH)}{d(t)} = a \cdot \text{EXP}[-b \cdot DH] \quad (2.30)$$

$$a = \frac{k_2 K_S e_0}{K_S S_0 + S_0^2} \quad (2.31)$$

$$b = \frac{k_3 K_M K_S}{k_2 [K_S + S_0]} \quad (2.32)$$

To estimate constants, equation **Error! Reference source not found.** and **Error! Reference source not found.** were linearized by using the double reciprocal approach of Hannes-Woolf. K_M (= 1.8963), K_S (= 456.75 g/L), k_2 (= 1.2191 min⁻¹), k_3 (= 0.1173 min⁻¹) were estimated, and the final model was obtained as following.

$$\frac{d(DH)}{d(t)} = \frac{101.59e_0}{456.75S_0 + S_0^2} \text{EXP} \left[-\frac{114.45}{456.75 + S_0} DH \right] \quad (2.33)$$

The proposed exponential kinetic equation provided good predictions with the low average relative-error value (ARE, 3.26%) [83].

Although there are kinetic studies of protein enzymatic hydrolysis in fish processing industries there is little study in mussel processing. Studies have focused on determining optimal reaction condition for enzymatic hydrolysis of mussel proteins. The reaction rate is required to provide essential engineering information for design and scale up.

2.6 Conclusions

Landfill disposal of WMS represents a loss of value and environmental and economic burden to mussel processors and harvesters. WMS is a rich source of bio-CaCO₃ and proteins, which can be utilized for numerous applications. Applications include calcium supplement for animal feed, soil amendment, wastewater treatment, filler in plastic industry, construction, catalyst, and hydroxyapatite production. In above mentioned studies, MS showed its ability to replace the mined calcium carbonate with equivalent or better performance. The mussel meat is also a source of proteins which can be used for food ingredients, supplements, stabilizers in beverages, natural flavors, antimicrobial agents, and a cardio-protective nutrient. However, the review shows the bulk of studies in WMS focus on the bio-CaCO₃, ignoring the residual meat. This meat will be present in discarded and unmarketable shells and will impact the feasibility of any shell applications. Further there is added value in recovering the meat. Using enzymatic hydrolysis to recover “clean” WMS is attractive due to the low energy requirements non-toxicity of the process, and ability to recover all value-added products. The enzymatic meat removal process is

impacted by many factors such as composition of substrates, enzymes used, reaction conditions, and the required quality of protein hydrolysates (based on application). This review shows that more work is needed in establishing these process parameters to both optimize the “cleanaing” process and determine the quality of the recovered protein. It is needed to choose a suitable method to develop a kinetic equation to model the enzymatic hydrolysis of mussel proteins.

REFERENCES

- [1] FAO, *FAO yearbook. Fishery and Aquaculture Statistics 2018*, vol. 5. 2020.
- [2] L. Pinotti, V. Dell'Orto, and IFFO, "IFFO Positional Statement," *Biotechnol. Agron. Soc. Environ.*, vol. 15, no. SPEC. ISSUE 1, pp. 9–14, 2013.
- [3] T. Cashion *et al.*, "A global fishing gear dataset for integration into the Sea Around Us global fisheries databases.," *Fish. Cent. Res. Reports*, vol. 26, no. 1, 2018.
- [4] H. Yang, L. N. Sturmer, and S. Baker, "Molluscan Shellfish Aquaculture and Production," pp. 1–8, 2016.
- [5] E. T. D. E. L. Aquaculture, *FAO Yearbook. Fishery and Aquaculture Statistics 2018/FAO annuaire. Statistiques des pêches et de l'aquaculture 2018/FAO anuario. Estadísticas de pesca y acuicultura 2018*. 2020.
- [6] F. M. Suplicy, "A review of the multiple benefits of mussel farming," *Rev. Aquac.*, vol. 12, no. 1, pp. 204–223, 2020.
- [7] Fishery and Ocean Canada, "Farmed Mussels," 2017. [Online]. Available: <https://www.dfo-mpo.gc.ca/aquaculture/sector-secteur/species-especes/mussels-moules-eng.htm>. [Accessed: 03-Jan-2020].
- [8] A. S. Naik and M. Hayes, "Bioprocessing of mussel by-products for value added ingredients," *Trends in Food Science and Technology*, vol. 92. Elsevier Ltd, pp. 111–121, 01-Oct-2019.
- [9] M. Tokeshi, N. Ota, and T. Kawai, "A comparative study of morphometry in shell-bearing molluscs," *J. Zool.*, vol. 251, no. 1, pp. 31–38, 2000.
- [10] J. N. Murphy and F. M. Kerton, "Characterization and utilization of waste streams from mollusc aquaculture and fishing industries," in *Fuels, Chemicals and Materials from the Oceans and Aquatic Sources*, F. M. Kerton and N. Yan, Eds.

John Wiley & Sons Ltd, 2017, pp. 189–225.

- [11] J. P. Morris, T. Backeljau, and G. Chapelle, “Shells from aquaculture : a valuable biomaterial , not a nuisance waste product,” pp. 42–57, 2019.
- [12] M. C. Barros, P. M. Bello, M. Bao, and J. J. Torrado, “From waste to commodity: transforming shells into high purity calcium carbonate,” *J. Clean. Prod.*, vol. 17, no. 3, pp. 400–407, Feb. 2009.
- [13] A. P. Jackson, J. F. V Vincent, R. M. Turner, and P. R. S. L. B, “The mechanical design of nacre,” *Proc. R. Soc. London. Ser. B. Biol. Sci.*, vol. 234, no. 1277, pp. 415–440, 1988.
- [14] L. Génio, S. Kiel, M. R. Cunha, J. Grahame, and C. T. S. Little, “Shell microstructures of mussels (Bivalvia: Mytilidae: Bathymodiolinae) from deep-sea chemosynthetic sites: Do they have a phylogenetic significance?,” *Deep. Res. Part I Oceanogr. Res. Pap.*, vol. 64, pp. 86–103, Jun. 2012.
- [15] C. Martínez-García, B. González-Fonteboa, D. Carro-López, and F. Martínez-Abella, “Impact of mussel shell aggregates on air lime mortars. Pore structure and carbonation,” *J. Clean. Prod.*, vol. 215, pp. 650–668, Apr. 2019.
- [16] B. Chen, X. Peng, J. G. Wang, and X. Wu, “Laminated microstructure of Bivalva shell and research of biomimetic ceramic/polymer composite,” *Ceram. Int.*, vol. 30, pp. 2011–2014, 2004.
- [17] A. P. Le Rossignol, S. G. Buckingham, S. E. G. Lea, and R. Nagarajan, “Breaking down the mussel (*Mytilus edulis*) shell: Which layers affect Oystercatchers’ (*Haematopus ostralegus*) prey selection?,” *J. Exp. Mar. Bio. Ecol.*, vol. 405, no. 1–2, pp. 87–92, Aug. 2011.
- [18] F. Nudelman, H. H. Chen, H. A. Goldberg, S. Weiner, and L. Addadi, “Spiers Memorial Lecture: Lessons from biomineralization: Comparing the growth

strategies of mollusc shell prismatic and nacreous layers in *Atrina rigida*,” *Faraday Discuss.*, vol. 136, pp. 9–25, 2007.

- [19] E. M. Gerhard *et al.*, “Design strategies and applications of nacre-based biomaterials,” *Acta Biomater.*, vol. 54, pp. 21–34, 2017.
- [20] M. H. Klünder, D. Hippler, R. Witbaard, and D. Frei, “Laser ablation analysis of bivalve shells - Archives of environmental information,” *Geol. Surv. Denmark Greenl. Bull.*, no. 15, pp. 89–92, 2008.
- [21] J. N. Murphy, C. M. Schneider, L. K. Mailänder, Q. Lepillet, K. Hawboldt, and F. M. Kerton, “Wealth from waste: Blue mussels (*Mytilus edulis*) offer up a sustainable source of natural and synthetic nacre,” in *Green Chemistry*, vol. 21, no. 14, Royal Society of Chemistry, 2019, pp. 3920–3929.
- [22] D. Chakrabarty and S. Mahapatra, “Aragonite crystals with unconventional morphologies,” *J. Mater. Chem.*, vol. 9, no. 11, pp. 2953–2957, 1999.
- [23] L. Jönsson and K. Elwinger, “Mussel meal as a replacement for fish meal in feeds for organic poultry - a pilot short-term study,” *Acta Agric. Scand. A Anim. Sci.*, vol. 59, no. 1, pp. 22–27, 2009.
- [24] A. Hart, “Mini-review of waste shell-derived materials’ applications,” *Waste Manag. Res.*, pp. 1–14, 2020.
- [25] R. W. Gerry, “Ground Dried Whole Mussels as a Calcium Supplement for Chicken Rations,” *Poult. Sci.*, vol. 59, no. 10, pp. 2365–2368, Oct. 1980.
- [26] C. McLaughlan, P. Rose, and D. C. Aldridge, “Making the Best of a Pest: The Potential for Using Invasive Zebra Mussel (*Dreissena Polymorpha*) Biomass as a Supplement to Commercial Chicken Feed,” *Environ. Manage.*, vol. 54, no. 5, pp. 1102–1109, 2014.
- [27] E. Álvarez, M. J. Fernández-Sanjurjo, N. Seco, and A. Núñez, “Use of Mussel

Shells as a Soil Amendment: Effects on Bulk and Rhizosphere Soil and Pasture Production,” *Pedosphere*, vol. 22, no. 2, pp. 152–164, 2012.

- [28] B. Garrido-Rodriguez *et al.*, “Competitive adsorption and transport of Cd, Cu, Ni and Zn in a mine soil amended with mussel shell,” *Chemosphere*, vol. 107, pp. 379–385, 2014.
- [29] D. Fernández-Calviño *et al.*, “Changes in Cd, Cu, Ni, Pb and Zn Fractionation and Liberation Due to Mussel Shell Amendment on a Mine Soil,” *L. Degrad. Dev.*, vol. 27, no. 4, pp. 1276–1285, 2016.
- [30] A. Núñez-Delgado *et al.*, “Cadmium and lead sorption/desorption on non-amended and by-product-amended soil samples and pyritic material,” *Water (Switzerland)*, vol. 9, no. 11, 2017.
- [31] A. Quintáns-Fondo *et al.*, “Promoting sustainability in the mussel industry: Mussel shell recycling to fight fluoride pollution,” *J. Clean. Prod.*, vol. 131, pp. 485–490, 2016.
- [32] C. Osorio-López *et al.*, “As(V) adsorption on forest and vineyard soils and pyritic material with or without mussel shell: Kinetics and fractionation,” *J. Taiwan Inst. Chem. Eng.*, vol. 45, no. 3, pp. 1007–1014, 2014.
- [33] N. Seco-Reigosa *et al.*, “Adsorption, desorption and fractionation of As(V) on untreated and mussel shell-treated granitic material,” *Solid Earth*, vol. 6, no. 1, pp. 337–346, 2015.
- [34] M. I. Jones, L. Y. Wang, A. Abeynaike, and D. A. Patterson, “Utilisation of waste material for environmental applications: calcination of mussel shells for waste water treatment,” *Adv. Appl. Ceram.*, vol. 110, no. 5, pp. 280–286, 2011.
- [35] L. Ji *et al.*, “Modified mussel shell powder for microalgae immobilization to remove N and P from eutrophic wastewater,” *Bioresour. Technol.*, vol. 284, pp.

36–42, Jul. 2019.

- [36] M. El Haddad *et al.*, “Calcined mussel shells as a new and eco-friendly biosorbent to remove textile dyes from aqueous solutions,” *J. Taiwan Inst. Chem. Eng.*, vol. 45, no. 2, pp. 533–540, 2014.
- [37] C. A. Papadimitriou, G. Krey, N. Stamatis, and A. Kallianiotis, “The use of waste mussel shells for the adsorption of dyes and heavy metals,” *J. Chem. Technol. Biotechnol.*, vol. 92, no. 8, pp. 1943–1947, Aug. 2017.
- [38] T. Ennil Bektaş, “Reduction dye in paint and construction chemicals wastewater by improved coagulation-flocculation process,” *Water Sci. Technol.*, vol. 76, no. 10, pp. 2816–2820, 2017.
- [39] S. Dandil, D. A. Sahbaz, and C. Acikgoz, “High performance adsorption of hazardous triphenylmethane dye-crystal violet onto calcinated waste mussel shells,” *Water Qual. Res. J. Canada*, vol. 54, no. 3, pp. 249–256, 2019.
- [40] F. Echabbi *et al.*, “Photocatalytic degradation of methylene blue by the use of titanium-doped Calcined Mussel Shells CMS/TiO₂,” *J. Environ. Chem. Eng.*, vol. 7, no. 5, Oct. 2019.
- [41] L. Cai *et al.*, “Preparation and evaluation of a hierarchical Bi₂MoO₆/MSB composite for visible-light-driven photocatalytic performance,” *RSC Adv.*, vol. 9, no. 65, pp. 38280–38288, 2019.
- [42] C. A. McCauley, A. D. O’Sullivan, M. W. Milke, P. A. Weber, and D. A. Trumm, “Sulfate and metal removal in bioreactors treating acid mine drainage dominated with iron and aluminum,” *Water Res.*, vol. 43, no. 4, pp. 961–970, 2009.
- [43] B. Uster *et al.*, “Waste Mussel Shells to Treat Acid Mine Drainage: A New Zealand Initiative,” *Am. Soc. Mining Reclam.*, no. October, pp. 23–27, 2014.
- [44] U. Yerlesen, “Studies on the properties of low density polyethylene composites

- filled seafood waste shell powder,” vol. 46, no. 1, pp. 43–48, 2016.
- [45] M. R. R. Hamester, P. S. Balzer, and D. Becker, “Characterization of calcium carbonate obtained from oyster and mussel shells and incorporation in polypropylene,” *Mater. Res.*, vol. 15, no. 2, pp. 204–208, Feb. 2012.
- [46] C. Koçhan, “Mechanical properties of waste mussel shell particles reinforced epoxy composites,” *Mater. Test.*, vol. 61, no. 2, pp. 149–154, 2019.
- [47] N. Nabilah Ismail, N. Hazurina Othman, G. Wan Inn, and M. Shabery Sainudin, “Physical and Mechanical Properties of Concrete Containing Green Mussel (*Perna viridis*) Shell Ash as an Admixture,” in *IOP Conference Series: Materials Science and Engineering*, 2019, vol. 601, no. 1.
- [48] C. Martínez-García, B. González-Fonteboa, F. Martínez-Abella, and D. Carro-López, “Performance of mussel shell as aggregate in plain concrete,” *Constr. Build. Mater.*, vol. 139, pp. 570–583, May 2017.
- [49] R. Rezaei, M. Mohadesi, and G. R. Moradi, “Optimization of biodiesel production using waste mussel shell catalyst,” *Fuel*, vol. 109, pp. 534–541, 2013.
- [50] B. Peceño, C. Arenas, B. Alonso-Fariñas, and C. Leiva, “Substitution of Coarse Aggregates with Mollusk-Shell Waste in Acoustic-Absorbing Concrete,” *J. Mater. Civ. Eng.*, vol. 31, no. 6, Jun. 2019.
- [51] A. Buasri, N. Chaiyut, V. Loryuenyong, P. Worawanitchaphong, and S. Trongyong, “Calcium Oxide Derived from Waste Shells of Mussel, Cockle, and Scallop as the Heterogeneous Catalyst for Biodiesel Production,” *Sci. World J.*, vol. 2013, 2013.
- [52] M. Mohadesi, G. Moradi, Y. Davvodbeygi, and S. Hosseini, “Soybean oil transesterification reactions in the presence of mussel shell: Pseudo-first order kinetics,” *Iran. J. Chem. Chem. Eng.*, vol. 37, no. 4, pp. 43–51, 2018.

- [53] M. I. Jones, H. Barakat, and D. A. Patterson, "Production of hydroxyapatite from waste mussel shells," in *IOP Conference Series: Materials Science and Engineering*, 2011, vol. 18, no. SYMPOSIUM 13.
- [54] R. Ramli, A. Z. O. Arawi, M. K. Talari, M. M. Mahat, and U. S. Jais, "Synthesis and structural characterization of nano-hydroxyapatite biomaterials prepared by microwave processing," *AIP Conf. Proc.*, vol. 1455, pp. 45–48, 2012.
- [55] A. Shavandi, A. E. D. A. Bekhit, A. Ali, and Z. Sun, "Synthesis of nano-hydroxyapatite (nHA) from waste mussel shells using a rapid microwave method," *Mater. Chem. Phys.*, vol. 149, pp. 607–616, 2015.
- [56] G. S. Kumar, E. K. Girija, M. Venkatesh, G. Karunakaran, E. Kolesnikov, and D. Kuznetsov, "One step method to synthesize flower-like hydroxyapatite architecture using mussel shell bio-waste as a calcium source," *Ceram. Int.*, vol. 43, no. 3, pp. 3457–3461, Feb. 2017.
- [57] M. Sari and Y. Yusuf, "Synthesis and characterization of hydroxyapatite based on green mussel shells (*perna viridis*) with the variation of stirring time using the precipitation method," *IOP Conf. Ser. Mater. Sci. Eng.*, vol. 432, no. 1, 2018.
- [58] S. Meski *et al.*, "Synthesis of hydroxyapatite from mussel shells for effective adsorption of aqueous Cd(II)," *Water Sci. Technol.*, pp. 1–12, 2019.
- [59] G. T. El-Bassyouni, S. H. Kenawy, R. S. Hassan, M. Mabrouk, and E. M. A. Hamzawy, "Removal of ^{137}Cs and $^{152+154}\text{Eu}$ Using Hydroxyapatite Prepared from Mussel Shells," *InterCeram Int. Ceram. Rev.*, vol. 68, no. 6, pp. 34–41, Oct. 2019.
- [60] J. H. Shariffuddin, M. I. Jones, and D. A. Patterson, "Greener photocatalysts: Hydroxyapatite derived from waste mussel shells for the photocatalytic degradation of a model azo dye wastewater," *Chem. Eng. Res. Des.*, vol. 91, no. 9, pp. 1693–1704, Sep. 2013.

- [61] S. Egerton, S. Culloty, J. Whooley, C. Stanton, and R. P. Ross, "Characterization of protein hydrolysates from blue whiting (*Micromesistius poutassou*) and their application in beverage fortification," *Food Chem.*, vol. 245, pp. 698–706, 2018.
- [62] S. He, C. Franco, and W. Zhang, "Functions, applications and production of protein hydrolysates from fish processing co-products (FPCP)," *Food Res. Int.*, vol. 50, no. 1, pp. 289–297, 2013.
- [63] S. Karnjanapratum and S. Benjakul, "Antioxidative and sensory properties of instant coffee fortified with galactose-fish skin gelatin hydrolysate maillard reaction products," *Carpathian J. Food Sci. Technol.*, vol. 9, no. 1, pp. 90–99, 2017.
- [64] S. Sinthusamran, S. Benjakul, K. Kijroongrojana, and T. Prodpran, "Chemical, physical, rheological and sensory properties of biscuit fortified with protein hydrolysate from cephalothorax of Pacific white shrimp," *J. Food Sci. Technol.*, vol. 56, no. 3, pp. 1145–1154, 2019.
- [65] A. T. Idowu and S. Benjakul, "Bitterness of fish protein hydrolysate and its debittering prospects," *J. Food Biochem.*, vol. 43, no. 9, pp. 1–10, 2019.
- [66] Y. Zhou, R. Thirumurugan, Q. Wang, C. M. Lee, and D. A. Davis, "Use of dry hydrolysate from squid and scallop product supplement in plant based practical diets for Pacific white shrimp *Litopenaeus vannamei*," *Aquaculture*, vol. 465, pp. 53–59, 2016.
- [67] R. Novriadi, E. Spangler, M. Rhodes, T. Hanson, and D. Allen Davis, "Effects of various levels of squid hydrolysate and squid meal supplementation with enzyme-treated soy on growth performance, body composition, serum biochemistry and histology of Florida pompano *Trachinotus carolinus*," *Aquaculture*, vol. 481, pp. 85–93, 2017.
- [68] V. M. Silva, K. J. Park, and M. D. Hubinger, "Optimization of the enzymatic

- hydrolysis of mussel meat,” *J. Food Sci.*, vol. 75, no. 1, 2010.
- [69] I. Normah, “produced in the presence of sodium tripolyphosphate and NaCl,” vol. 25, no. December, pp. 2524–2530, 2018.
- [70] Z. Xu *et al.*, “Nutritional properties and osteogenic activity of enzymatic hydrolysates of proteins from the blue mussel (*Mytilus edulis*),” *Food Funct.*, vol. 10, no. 12, pp. 7745–7754, 2019.
- [71] Z. Dong *et al.*, “Antioxidant activities of peptide fractions derived from freshwater mussel protein using ultrasound-assisted enzymatic hydrolysis,” *Czech J. Food Sci.*, vol. 35, no. 4, pp. 328–338, 2017.
- [72] E. K. Kim *et al.*, “Purification of a novel anticancer peptide from enzymatic hydrolysate of *Mytilus coruscus*,” *J. Microbiol. Biotechnol.*, vol. 22, no. 10, pp. 1381–1387, 2012.
- [73] M. Qiao *et al.*, “Identification and antithrombotic activity of peptides from blue mussel (*Mytilus edulis*) protein,” *Int. J. Mol. Sci.*, vol. 19, no. 1, 2018.
- [74] L. Beaulieu, J. Thibodeau, C. Bonnet, P. Bryl, and M.-E. Carbonneau, “Evidence of Anti-Proliferative Activities in Blue Mussel (*Mytilus edulis*) By-Products,” *Mar. Drugs*, vol. 11, no. 12, pp. 975–990, Mar. 2013.
- [75] F. Nagel, T. Appel, C. Rohde, and E. Al., “Blue Mussel Protein Concentrate Versus Prime Fish Meal Protein as a Dietary Attractant for Turbot (*Psetta maxima* L.) Given Rapeseed Protein-based Diets,” *J. Aquac. Res. Dev.*, 2017.
- [76] M. J. Frude, “Method for removing excess meat from whole of crushed mollusk shellfish waste, New Zealand Pat.,” 555418, 2008.
- [77] J. N. Murphy, K. Hawboldt, and F. M. Kerton, “Enzymatic processing of mussel shells to produce biorenewable calcium carbonate in seawater,” *R. Soc. Chem.*, vol. 20, pp. 2913–2920, 2018.

- [78] A. S. Naik, L. Mora, and M. Hayes, “Characterisation of seasonal mytilus edulis by-products and generation of bioactive hydrolysates,” *Appl. Sci.*, vol. 10, no. 19, pp. 1–21, 2020.
- [79] L. J. G. Sampedro, N. A. G. Grimaldos, J. A. Pereañez, and J. E. Z. Montoya, “Lipids as competitive inhibitors of subtilisin Carlsberg in the enzymatic hydrolysis of proteins in red tilapia (*Oreochromis sp.*) Viscera: Insights from kinetic models and a molecular docking study,” *Brazilian J. Chem. Eng.*, vol. 36, no. 2, pp. 647–655, 2019.
- [80] V. Y. Novikov, S. R. Derkach, Y. A. Kuchina, A. Y. Shironina, and V. A. Mukhin, “Kinetics of enzymatic reactions in the production of fish protein hydrolysates,” *J. Dispers. Sci. Technol.*, vol. 0, no. 0, pp. 1–8, 2018.
- [81] Y. Tan, S. K. C. Chang, and S. Meng, “Comparing the kinetics of the hydrolysis of by-product from channel catfish (*Ictalurus punctatus*) fillet processing by eight proteases,” *Lwt*, vol. 111, no. February, pp. 809–820, 2019.
- [82] Q. Wei and H. Zhimin, “Enzymatic hydrolysis of protein : mechanism and kinetic model,” vol. 38, pp. 308–314, 2006.
- [83] J. E. Zapata Montoya, D. E. Giraldo-Rios, and A. J. Baéz-Suarez, “Kinetic modeling of the enzymatic hydrolysis of proteins of viscera from red tilapia (*Oreochromis sp.*): Effect of substrate and enzyme concentration,” *Vitae*, vol. 25, no. 1, pp. 17–25, 2018.

CHAPTER 3 – MATERIALS & EXPERIMENTS

3.1 Experimental

3.1.1 Materials

Blue mussels (*Mytilus edulis*) are the source of protein for the enzymatic hydrolysis in this study. Three types of mussels are used in the study: (i) marketable size mussels, and unmarketable size (ii) under sized, and (iii) oversized mussels. All market size mussels are purchased from the same grocery store (Sobeys, Merrymeeting Road, St John's, NL) and were of Newfoundland origin. Marketable mussels are 15-19 g per mussel. Oversized and undersized mussels were supplied by Sunrise Fish Farms Inc (Newfoundland and Labrador). Oversized mussels are approximately 22-23 g/mussel. Undersized mussels are in the range of 10-11g/mussel, **Error! Reference source not found..**



Figure 3 - 1: Mussels of different sizes

Mussels are pre-treated to eliminate organic compounds and visible outside beards on the shells and then classified into four different groups according to their size: 10-11 g (G-I),

15-16 g, (G-II), 18-19 g, (G-III), and 22-23g, (G-IV). Mussels are stored in Ziploc bags at -30 °C. Note G-I and G-IV are the under and over sized mussels.

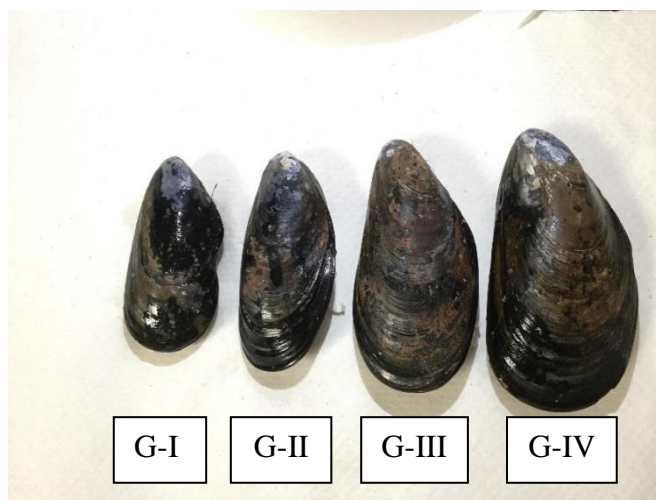


Figure 3 - 2: Pre-treated mussels

Multifect PR 6L (6L) enzyme was supplied by DuPont (Industrial Bioscience Division) and used to hydrolyze mussel meat in the study. 6L enzyme is a bacterial alkaline serine endopeptidase, derived from a strain of *Bacillus licheniformis*, with molecular weight 22.5 kDa. 6L enzyme is a brown liquid product food grade enzyme with an activity of 2440 ELU mL⁻¹ and is effective in hydrolyzing most proteins to lower molecular weight peptides [1]. The pH range for 6L enzyme activity is 7.0-10.0, with an optimum performance at pH 9.5. The temperature range for enzyme activity is from 25 °C - 70 °C, with an optimum temperature of 60°C (140 °F). However, overall optimum activity depends on several process variables, including temperature, time, enzyme concentration, substrate concentration, and substrate composition. The price of 6L enzyme on the market was 185 CAD / 250 mL when the study was carried out [1].

As mentioned above, 6L enzyme is active over a wide range of pH, from neutral to alkaline. It also has a reasonable price for use on an industrial scale. In screening studies 6L performed well in tap water in hydrolysis of the mussel shells [2]. As such, in this study, experiments are carried out in tap water. The pH value of tap water is checked randomly through a day for a week, **Error! Reference source not found.** The results showed that the pH of tap water is neutral and stable.

Table 3 - 1: pH of tap water (City water) in St. John's, Newfoundland

| | 8.00 am | 12.00 pm | 4.00 pm | 7.00 pm |
|-------|---------|----------|---------|---------|
| Day 1 | 7.11 | 7.11 | 7.13 | 7.07 |
| Day 2 | 7.14 | 7.01 | 7.03 | 7.08 |
| Day 3 | 7.12 | 7.1 | 7.06 | 7.03 |
| Day 4 | 7.05 | 7.12 | 7.12 | 7.04 |
| Day 5 | 7.07 | 7.13 | 7.14 | 7.11 |
| Day 6 | 7.18 | 7.1 | 7.08 | 7.09 |
| Day 7 | 7.14 | 7.1 | 7.1 | 7.12 |

3.1.2 Equipment

Thermo Scientific™ MaxQ™ 4450 Benchtop Orbital Shakers was used to maintain constant temperatures and tiring speed for the enzymatic hydrolysis reactions. A 4-digit

analytical balance is used to weigh the samples. An EppendorfTM Research plusTM Variable Adjustable Volume Pipette is used to measure the amount of enzyme solution required.

3.1.3 Enzymatic hydrolysis of whole raw mussels using Multifect PR 6L enzyme

The enzymatic hydrolysis is conducted for whole raw mussels using Multifect PR 6L enzyme. The optimum conditions for the hydrolysis of mussel meat using 6L enzyme were determined in previous studies: tap water, temperature of 50 °C, neutral and non-adjusted pH [2][3]. The initial enzyme and substrate concentration are varied to study the effect on the hydrolysis rate and extent. The initial enzyme concentration (E_o , $\mu\text{L/L}$) is defined as the volume of the enzyme (μL) divided by volume of tap water (L). The concentration of substrate (S_o , g/L) is the mass of whole mussels (g) per L tap water. In the first set of experiments, the initial enzyme concentration is varied from 62 $\mu\text{L/L}$ to 250 $\mu\text{L/L}$ on marketable mussels (initial meat/substrate concentration of 125 g/L) or G-II. In the second set, the impact of mussel size/meat is tested or G-I, III, and IV. The initial enzyme concentration is fixed at 125 $\mu\text{L/L}$ for these experiments and initial substrate concentration varies from 100 g/L to 175 g/L. All experiments were run in triplicate for a total of 21 experiments.

Table 3 - 2: Initial enzyme and substrate concentration for experiments

| | Varying E_o | | | | Varying S_o (Mussel size) | | | |
|---------------------------|---------------|-----|-----|-----|-----------------------------|-----|-----|-----|
| E_o ($\mu\text{L/L}$) | 62 | 125 | 188 | 250 | 125 | 125 | 125 | 125 |

| | | | | | | | | |
|---------------|------|------|------|------|-----|------|-------|------|
| S_o (g/mL) | 125 | 125 | 125 | 125 | 100 | 125 | 150 | 175 |
| Mussels group | G-II | G-II | G-II | G-II | G-I | G-II | G-III | G-IV |

Whole raw frozen mussels were thawed over 2 h. Mussel shells then opened naturally. The outside and inside beards are eliminated by hand, **Error! Reference source not found. i).**

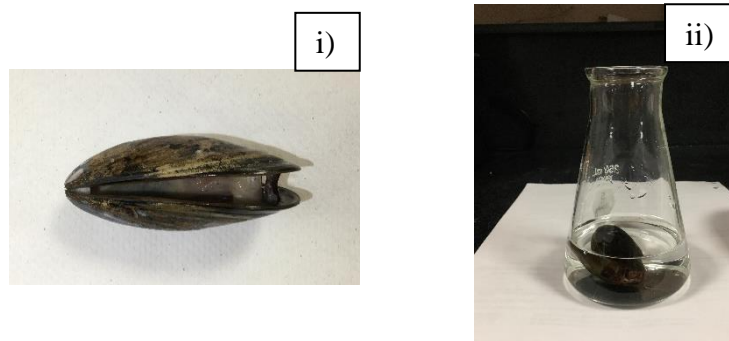


Figure 3 - 3: Defrosted mussels i) and the flask containing mussels ii)

The hydrolysis experiments of whole raw mussels were conducted in a 250 mL wide-neck Erlenmeyer flask. Pre-treated mussels are weighed (m_o) and placed in the flask. A measured amount of tap water is added into the flasks. The flasks containing mussels and tap water were heated up in a Qmax 4500 incubator to 50 °C for 30 min (**Error! Reference source not found. ii).** The enzyme is then added at time 0. At the specified sampling time, mussel samples are taken out, gently rinsed under cold tap water for 2 min, and then placed

in the fridge for 2 h to dry, **Error! Reference source not found.** The hydrolysate solution was put back in the incubator until the end of the experiment.

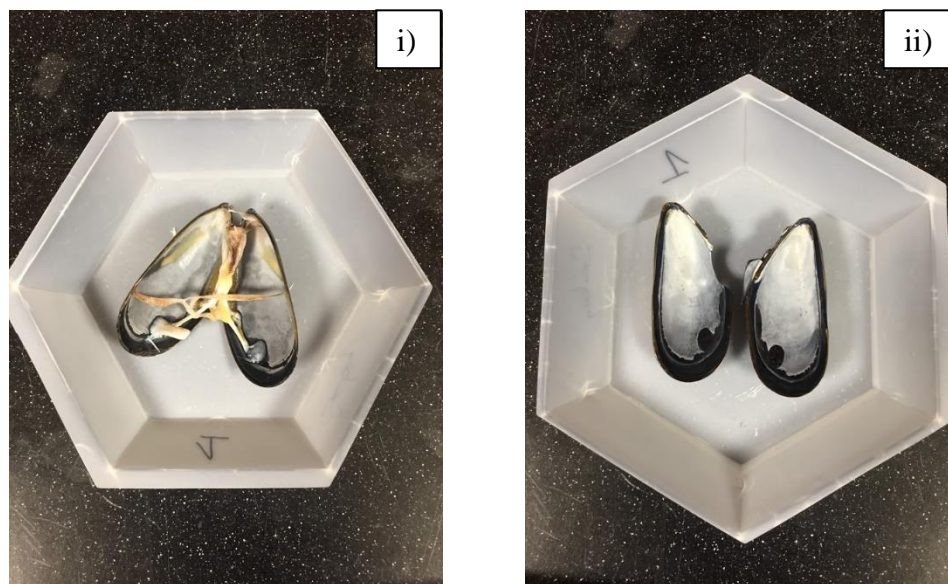


Figure 3 - 4: Mussel with leftover meat after hydrolysis i), and cleaned mussel shells after reaction ii)

The mass of mussels sampled is weighted (m_t). Any meat left on the sampled shells is removed manually and the mass of the meat free mussel shell (m_{shell}) is measured. The protein hydrolysate is heated to 80 °C to deactivate the enzyme. The protein hydrolysate is centrifuged to remove large impurities before being stored in the freezer at -30 °C for further analysis.

3.1.4 Degree of digested meat

Enzymatic hydrolysis is a process in which enzymes facilitate the cleavage of bonds in protein molecules to reduce protein molecular weight (peptides). The performance of

the enzymatic hydrolysis is typically evaluated via the degree of hydrolysis (DH) which is defined as the proportion of cleaved peptide bonds in a protein hydrolysate.

$$\text{DH (\%)} = \frac{h}{h_{\text{tot}}} \times 100 \quad (3.1)$$

Where h is the number of hydrolyzed peptide bonds and h_{tot} is the total number of peptide bonds present. The most common methods used to determine DH including the pH-stat, trinitrobenzenesulfonic acid (TNBS), o-phthalaldehyde (OPA), and formol titration methods [4]. The pH-stat method is the simplest which bases on the number of protons released during hydrolysis [4]. The TNBS, OPA, and formol titration methods are based on the generation of amino groups during the hydrolysis [4]. The accuracy of these methods is affected by the type of hydrolytic enzymes used, the size of the hydrolyzed peptides, and the reaction condition [4].

In this study, the enzymatic hydrolysis of whole raw mussels is conducted without pH control, so it is not possible to determine the DH by the pH-stat method. In addition, whole raw mussels contain many impurities (organic compounds and mussel beards), so it is not an ideal environment for titrating the concentration of the generated amino groups.

The concept of the degree of digested meat (DM) is developed in this study. The digestion of mussel meat means that the insoluble protein in mussel meat is turned into soluble protein in hydrolysate by the cleavage of peptide bonds. The degree of digested meat is defined as the ratio of digested mussel meat to the total mussel meat. In effect the degree

of digested meat is an estimation of DH, while it may not capture the protein cleavage to the smallest peptide, it does reflect the cleavage of the meat from the shell. In this study, the efficiency of the enzymatic cleaning of the shells will be evaluated via the DM instead of the DH.

$$DM(t) = \frac{\Delta m_{\text{meat}}}{m_{\text{meat}}} = \frac{m_o - m_t}{m_o - m_{\text{shell}}} \quad (3.2)$$

Where $DM(t)$ is the degree of digested meat at time t , Δm_{meat} is the weight of digested meat (g), m_{meat} is the total weight of meat (g), m_o is the total weight of whole mussel (g), m_t is the weight of the whole mussel at time t (g), m_{shell} is the weight of mussel shells (g).

To calculate the DM, one needs to know m_o , m_{shell} , and m_t . To determine m_t , seven mussels, selected based on similarity in weight and size, are used to represent seven different sampling points over the 150 min of the hydrolysis experiment, and labelled sample one (S1) through to seven (S7). All samples 1-7 are placed in the incubator at the same time, marking the start of the experiment. Sample S1 ($m_{o,S1}$) is removed at 10 min. and weighted ($m_{t,S1}$) following the procedure outlined above. All leftover meat on sample S1 is removed manually to determine the mass of shells in S1 ($m_{\text{shell},S1}$). This procedure is repeated for S2, when the sample is removed at the next time interval, and this continues until S7 (150 minutes for this set of experiments). The DM at certain time points is calculated from the obtained information. Finally, the DM curves are plotted as a function of time. This procedure was followed as taking samples from the same flask with time

would complicate the measurement of the rate as the mass of meat would be changing with each sampling interval.

Table 3 - 3: Arrange of prepared samples for one experiment

| Sample | S1 | S2 | S3 | S4 | S5 | S6 | S7 | S8 |
|--------------------|-----------------|-----------------|-----------------|-----------------|-----------------|-----------------|-----------------|-----------------|
| Initial mass (g) | m_{o_S1} | m_{o_S2} | m_{o_S3} | m_{o_S4} | m_{o_S5} | m_{o_S6} | m_{o_S7} | m_{o_S8} |
| Time (min) | 10 | 20 | 30 | 40 | 60 | 80 | 110 | 150 |
| Mass at time t (g) | m_{t_S1} | m_{t_S2} | m_{t_S3} | m_{t_S4} | m_{t_S5} | m_{t_S6} | m_{t_S7} | m_{t_S8} |
| Mass of shells (g) | m_{shell_S1} | m_{shell_S2} | m_{shell_S3} | m_{shell_S4} | m_{shell_S5} | m_{shell_S6} | m_{shell_S7} | m_{shell_S8} |
| DM | DM_{S1} | DM_{S2} | DM_{S3} | DM_{S4} | DM_{S5} | DM_{S6} | DM_{S7} | DM_{S8} |

3.2 Kinetic models for enzymatic hydrolysis of fish protein:

The hydrolysis is conducted on the entire mussel instead of ground mussel meat, so it could be considered a heterogeneous reaction. Therefore, the rate of hydrolysis is affected by the hydrolysis mechanism (e.g. inhibition, competition etc.), mixing efficiency, contact area of enzyme and substrate, diffusion, and types of protein in mussel meat. This study aims to develop a kinetic model to predict the DM as a function of time as a function of initial substrate and enzyme concentration. As outlined in chapter 2, kinetic models developed to

predict DH are modified to predict DM instead of DH. All three models reviewed in chapter 2 would be tested for experiment data in this study.

The Peleg model was investigated for predicting the DH of the hydrolysis of channel catfish (*Ictalurus punctatus*) by-product using a range of enzymes at different reaction conditions [5].

$$DH(t) = \frac{t}{K_1 + K_2 \cdot t} \quad (3.3)$$

Where DH (t) (%) is the degree of hydrolysis at time t, t is the hydrolysis time (min), K₁ is Peleg's rate constant relating to the degree of hydrolysis at the very beginning, and K₂ is Peleg's capacity constant relating to a maximum degree of hydrolysis. In this study, the variable DM is substituted for DH and the Peleg equation predicting the DM of the hydrolysis of mussel is indicated as followed.

$$DM(t) = \frac{t}{K_1 + K_2 \cdot t} \quad (3.4)$$

Marquez and Fernandez proposed an exponential model which was later modified by Gonzalez-Tello and Camacho to describe the hydrolysis of vegetable and whey proteins in a batch reactor [6].

$$\frac{d(DH)}{d(t)} = a. \text{EXP}[-b. DH] \quad (3. 5)$$

The integrated form of equation **Error! Reference source not found.** is a logarithmic equation as followed.

$$DH = \frac{1}{b} \ln (1 + abt) \quad (3. 6)$$

Where DH (t) (%) is the degree of hydrolysis at time t, 'a' and 'b' are kinetic parameters. 'a' and 'b' consist of a group of kinetic constants which depend on the kinetic mechanisms, which was published by Qi and He [7]. For different mechanisms, it could be observed that 'a' depends on the initial enzyme and substrate concentration, while 'b' only depends on the initial substrate concentration.

In this work, it is implied the substitution of the DM for the DH. The variable DM was used instead of DH, as indicated in following equations.

$$\frac{d(DM)}{d(t)} = a. \text{EXP}[-b. DM] \quad (3. 7)$$

$$DM = \frac{1}{b} \ln (1 + abt) \quad (3. 8)$$

The final model is selected to fit experimental data is the first-order kinetic model. This model was investigated for the enzymatic hydrolysis of waste products of Atlantic cod (*Gadus morhua*) processing at different initial substrate and enzyme concentrations by using an enzyme specimen hepatopancreatine [8]. Amino nitrogen is a product of enzymatic hydrolysis. The enzymatic hydrolysis efficiency could be estimated by the accumulation of amino nitrogen in the hydrolysate instead of the DH. An assumption of a first-order reaction and no enzyme autolysis during the reaction, the equation **Error! Reference source not found.** was used to predict the amino nitrogen accumulation with time.

$$C_A = C_{A\infty}(1 - e^{-kt}) \quad (3.9)$$

Where C_A is the amino nitrogen concentration at time t , $C_{A\infty}$ is the value of C_A at $t \rightarrow \infty$, k is the rate constant, and t is time (min). The model did not fit the experimental data for the entire length of the experiment due to enzyme autolysis and the substrate inhibition. However, it could be used to fit the experimental data of the enzymatic hydrolysis of mussels because it is assumed that there is not enzyme autolysis or any inhibition in the hydrolysis process of mussels. This assumption based on the composition of mussel meat which mainly contains water and protein. The content of lipid which could be an inhibitor of in mussel meat is very low, less than 2 wt.% [9].

$$DM = DM_{\infty}(1 - e^{-kt}) \quad (3.10)$$

3.3 Characterizations analysis - Solubilized protein concentration of hydrolysate

Solubility is the an important functional property of a protein hydrolysate as this parameter relates to many different properties such as surface hydrophobic (protein–protein) or hydrophilic (protein–solvent) interaction [10][11]. After hydrolysis, the hydrolysates of mussel meat were more soluble than native proteins. The hydrolysates are a value-added by-product which could be utilized in fishmeal industry.



Figure 3 - 5: Mussel proteins hydrolysate

As stated above, it was observed that most of protein in the obtained hydrolysates were soluble, as such the Bio-Rad Protein Assay based on the method of Bradford method was used to determine concentration of these solubilized proteins. The hydrolysate does not contain any interfering agents which could potentially affect the results of the Bio-Rad Protein Assay. The Bio-Rad Protein Assay is a dye-binding assay which measures various concentrations of protein based on a differential color change of a dye. This analysis was performed for all obtained hydrolysates at different reaction condition.

REFERENCES

- [1] D. Bacterial and A. Protease, “Multifect® pr 6l.”
- [2] J. N. Murphy, K. Hawboldt, and F. M. Kerton, “Enzymatic processing of mussel shells to produce biorenewable calcium carbonate in seawater,” *R. Soc. Chem.*, vol. 20, pp. 2913–2920, 2018.
- [3] V. M. Silva, K. J. Park, and M. D. Hubinger, “Optimization of the enzymatic hydrolysis of mussel meat,” *J. Food Sci.*, vol. 75, no. 1, 2010.
- [4] S. M. Rutherford, “Methodology for determining degree of hydrolysis of proteins in hydrolysates: A Review,” *J. AOAC Int.*, vol. 93, no. 5, pp. 1515–1522, 2010.
- [5] Y. Tan, S. K. C. Chang, and S. Meng, “Comparing the kinetics of the hydrolysis of by-product from channel catfish (*Ictalurus punctatus*) fillet processing by eight proteases,” *Lwt*, vol. 111, no. February, pp. 809–820, 2019.
- [6] P. L. Valencia *et al.*, “Proteolytic susceptibility of food by-product proteins: An evaluation by means of a quantitative index,” *Process Biochem.*, vol. 77, no. August 2018, pp. 63–69, 2019.
- [7] Q. Wei and H. Zhimin, “Enzymatic hydrolysis of protein : mechanism and kinetic model,” vol. 38, pp. 308–314, 2006.
- [8] V. Y. Novikov, S. R. Derkach, Y. A. Kuchina, A. Y. Shironina, and V. A. Mukhin, “Kinetics of enzymatic reactions in the production of fish protein hydrolysates,” *J. Dispers. Sci. Technol.*, vol. 0, no. 0, pp. 1–8, 2018.
- [9] S. Dernekbaşı, “The Fatty Acid Composition of Cultured Mussels (*Mytilus galloprovincialis* Lamarck 1819) in Offshore Longline System in the Black Sea,” *J. Aquac. Mar. Biol.*, vol. 2, no. 6, 2015.
- [10] M. R. Segura-Campos, L. Espinosa-García, L. A. Chel-Guerrero, and D. A.

Betancur-Ancona, “Effect of Enzymatic Hydrolysis on Solubility, Hydrophobicity, and *In Vivo* Digestibility in Cowpea (*Vigna unguiculata*),” *Int. J. Food Prop.*, vol. 15, no. 4, pp. 770–780, Jul. 2012.

- [11] G. Leni, L. Soetemans, A. Caligiani, S. Sforza, and L. Bastiaens, “Degree of hydrolysis affects the techno-functional properties of lesser mealworm protein hydrolysates,” *Foods*, vol. 9, no. 4, 2020.

CHAPTER 4 – RESULTS AND DISCUSSION

4.1 Effect of the initial enzyme and mussel age (or substrate concentration) on hydrolysis of raw marketable mussel

In this section, the effect of the initial enzyme (E_o) and substrate (S_o) concentration on the hydrolysis of whole raw mussels (marketable) is discussed. The extent of hydrolysis is captured in measurement of the DM at a constant temperature of 50 °C and neutral pH.

To assess the significance of the effect of E_o and S_o on the DM an analysis of variance (ANOVA) is used. At a constant S_o of 125 g/L, E_o was varied from 62 to 250 μ L/L and ANOVA used to compare the DM over the hydrolysis period (Table 4 - 1). For the experiments where S_o was varied, the E_o was set at 125 μ L/L (Table 4 - 2).

Table 4 - 1: ANOVA of the DM when hydrolyzing mussels at different E_o

| Time (min) | Fraction of DM Mean square | p-value |
|------------|-------------------------------|---------|
| 10 | 0.0078 | 3.9E-07 |
| 20 | 0.0596 | 4.5E-10 |
| 30 | 0.0751 | 6.1E-10 |
| 40 | 0.1088 | 3.9E-10 |
| 60 | 0.1037 | 2.2E-10 |

| | | |
|-----|--------|---------|
| 80 | 0.0715 | 2.4E-10 |
| 110 | 0.0510 | 2.7E-09 |
| 150 | 0.0496 | 1.3E-10 |

Table 4 - 2: ANOVA of the DM when hydrolyzing mussels at different S_0 .

| Time (min) | Fraction of DM Mean square | p-value |
|------------|-------------------------------|---------|
| 10 | 0.00425 | 7.6E-06 |
| 20 | 0.00561 | 1.9E-06 |
| 30 | 0.00561 | 1.9E-06 |
| 40 | 0.04711 | 6.5E-10 |
| 60 | 0.03560 | 1.6E-09 |
| 80 | 0.03126 | 4.0E-09 |
| 110 | 0.06667 | 5.5E-06 |
| 150 | 0.04711 | 6.5E-10 |

The p-values represent the probability that E_0 and S_0 impact the final DM. The p-values indicate that both the initial enzyme and substrate concentration have a significant effect on DM over the entire hydrolysis period as p-values are less than 0.05.

Error! Reference source not found. summarizes the DM as a function of E_0 and time. As E_0 increases from 62 $\mu\text{L/L}$ to 250 $\mu\text{L/L}$, or $E_0:S_0$ increases from 0.5 $\mu\text{L/g}$ to 2.0 $\mu\text{L/g}$, the DM increases and reaches values close to 95%. The results imply that the DM during enzymatic protein hydrolysis is proportional to E_0 . This is not unexpected as enzymes represents “sites” for reaction so as enzyme concentration increases there are more available active reaction sites.

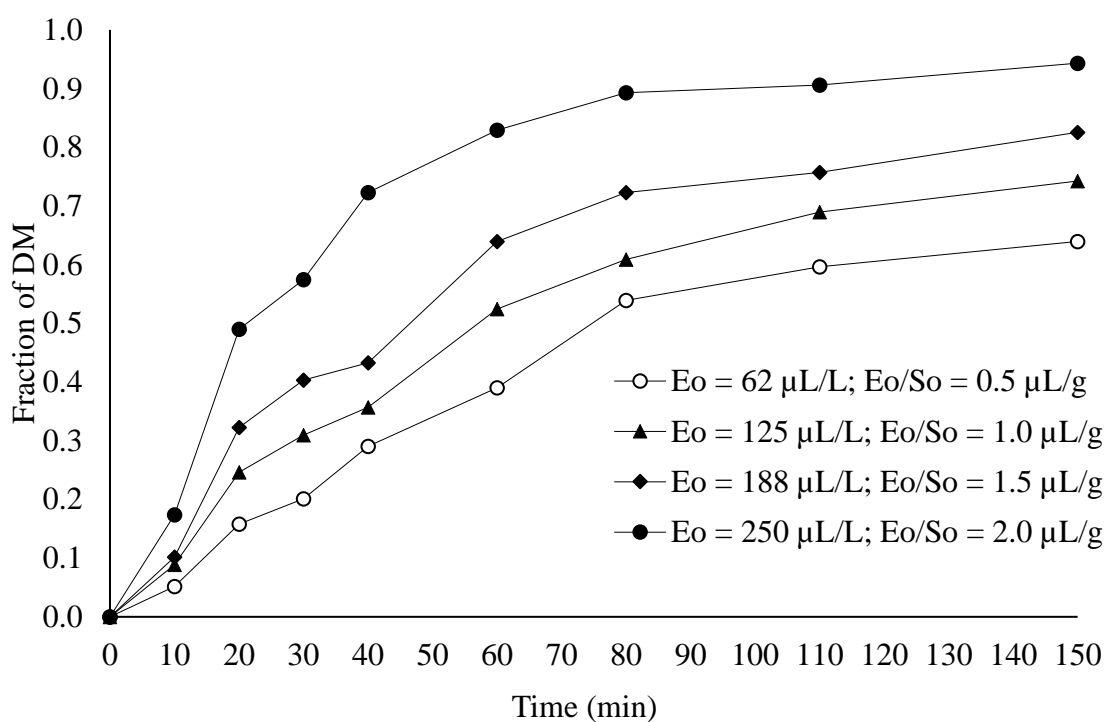


Figure 4 - 1: The fraction of DM during the hydrolysis period under different initial enzyme concentration ($S_0 = 125 \text{ g/L}$, $T = 50 \text{ }^\circ\text{C}$, Neutral pH, 160rpm)

Error! Reference source not found. outlines the DM as the function of S_o and time. Increases in S_o reduces the DM or the DM is inversely proportional to S_o . Given the amount of meat is increasing this is expected as the ratio of $E_o:S_o$ governs the rate of reaction.

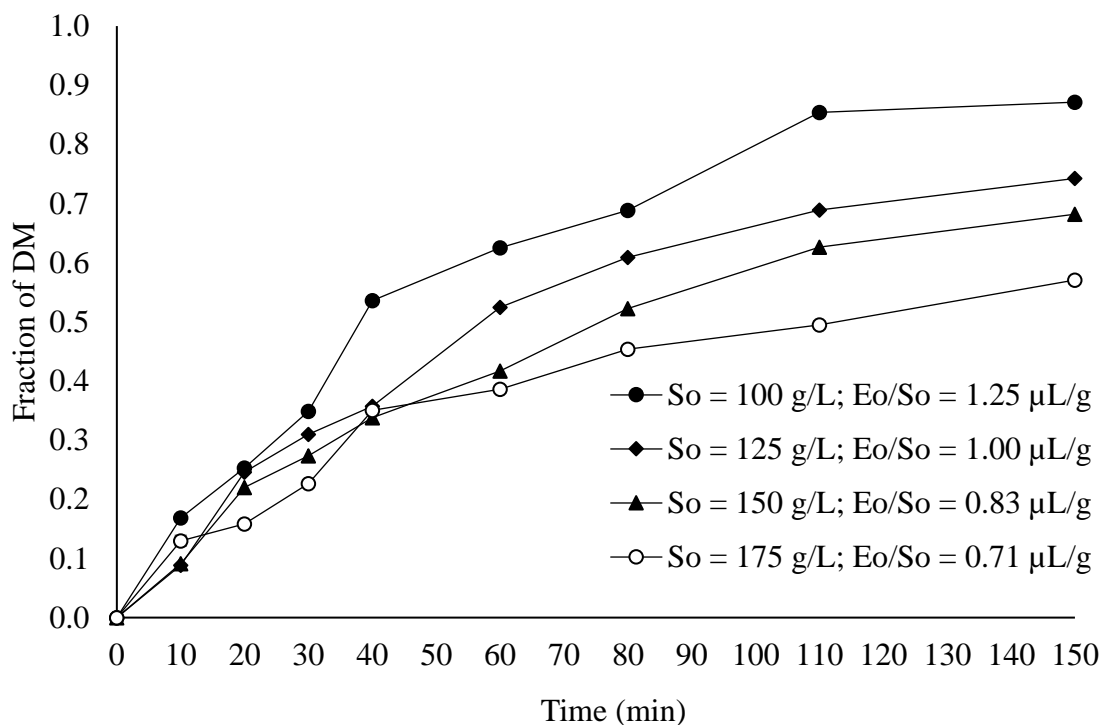


Figure 4 - 2: The fraction of DM during the hydrolysis period under different initial substrate concentration ($E_o = 125 \mu\text{L/L}$, $T = 50 \text{ }^\circ\text{C}$, Neutral pH, 160rpm)

It should be noted at the low $E_o:S_o$ ratios (e.g., $E_o:S_o < 1.25 \mu\text{L/g}$), the DM potentially could continue increasing as demonstrated in the experiments carried out past 150 min, Figure 4 - 12. whereas $E_o:S_o \geq 1.25 \mu\text{L/g}$ the DM appears to flatten out in 150 min. The impact of this will be discussed in more detail later. In addition to the $E_o:S_o$ ratio, there are other factors that impact the rate and DM. For the above experiments, whole raw mussels (with meat) were used, and first stage of hydrolysis the reaction occurs only on the surface of

mussel meat. In addition, the adductors hold two parts of the mussel shells quite close together, as the reaction proceeds the adductors are hydrolyzed. As such, initially the rates of reaction and DM are less dependent on the $E_o:S_o$ and as the adductors breakdown the mussel opens, and the DM is driven by $E_o:S_o$.

These results are important as higher values of DM may be associated with the quality and nutritional value of the hydrolysate in addition to the performance of the removal process [1]. The higher DM reflects the hydrolysis of the larger insoluble proteins to more soluble lower molecular weight peptides, which are required for food products, but does not reflect the proportion of protein bonds cleaved relative to the total number of bonds that could be cleaved or available for hydrolysis (defined as degree of hydrolysis).

In summary, both E_o and S_o have an effect on the final DM, and the rate of the hydrolysis. DM is also related to the chemistry of the obtained hydrolysate and as well as an indicator of rate of hydrolysis.

4.2 Model validation for the enzymatic hydrolysis of whole raw marketable size mussels

In this section, the models outlined in chapter three are tested. The relation between kinetic constants and the $E_o:S_o$ ratio is also assessed. The model prediction and the results of experiments are compared to determine the most suitable model. It should be noted the data from very large oversize or aged mussels ($S_o = 175$ g/L) was not used as it was observed in these experiments many large pieces of insoluble mussel meat were suspended in hydrolysate which would skew the measured DM.

4.2.1 The Peleg equation (1988)

The Peleg equation is outlined below and has been modified for DM (vs DH):

$$DM = \frac{t}{K_1 + K_2 \cdot t} \quad (4.1)$$

Where DM (t) is the DM at time t, t is the hydrolysis time (min), K_1 is Peleg's rate constant relating to the DM at the initial stages of hydrolysis, and K_2 is Peleg's capacity constant relating to the maximum DM. A lower K_1 translates to higher DM in the initial stage of the hydrolysis. A lower K_2 translate to a higher final DM. So, the lower K_1 and K_2 would mean higher hydrolysis rates. Again, in this study, we are using DM as a surrogate for DH.

$$t \rightarrow 0: \quad DM \sim \frac{t}{K_1} \quad (4.2)$$

$$t \rightarrow \infty: \quad DM \sim \frac{1}{K_2} \quad (4.3)$$

Peleg's equation (4. 1) is used to fit hydrolysis curves under various conditions of E_o and S_o . The results are shown in Figure 4 - 4 and Figure 4 - 3.

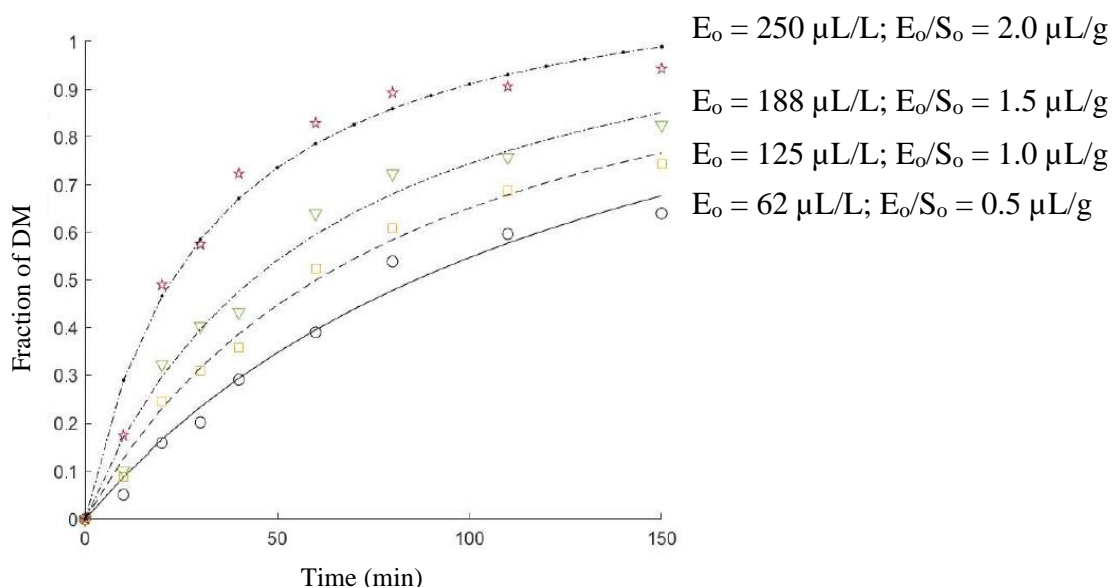


Figure 4 - 4: Kinetic curves for the fraction of DM. Symbols represent for experimental data; lines are the Peleg model predictions. The concentrations of the enzyme are indicated in the curves. $S_o = 125$ g/L

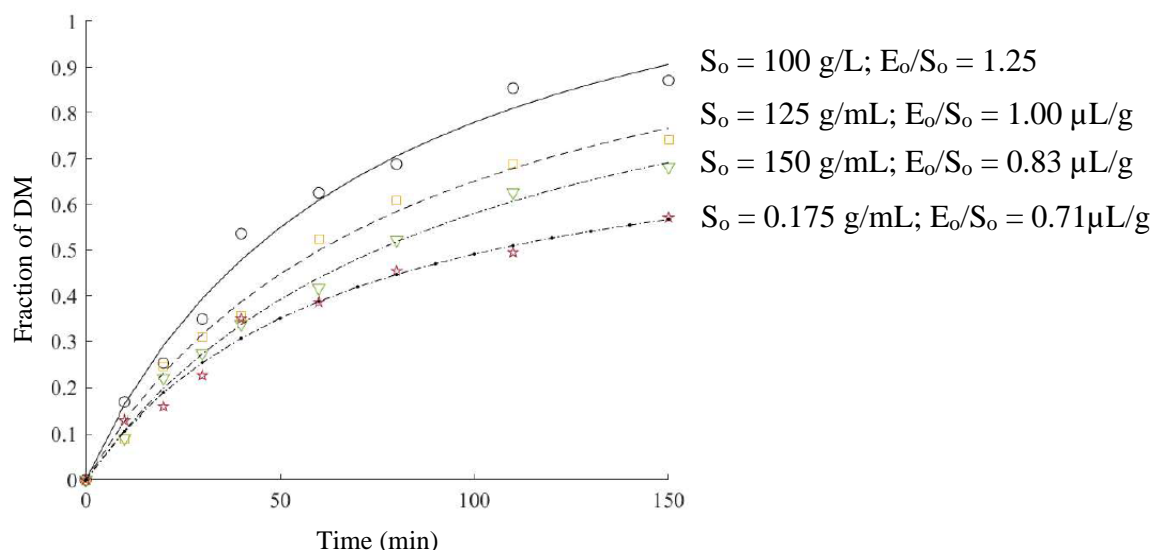


Figure 4 - 3: Kinetic curves for the fraction of DM. Symbols represent for experimental data; lines are the Peleg model predictions. The concentrations of the substrate are indicated in the curves. $E_o = 125$ μL/L

The data fit the Peleg equation well, having all R^2 higher than 0.97. Peleg's constants, K_1 and K_2 , are estimated and shown in

Table 4 - 3. The lowest K_1 is obtained at E_o of 250 $\mu\text{L/L}$ and S_o of 125 g/L at which it has the highest rate of hydrolysis in the initial stage. The lowest K_2 is at E_o of 125 $\mu\text{L/L}$ and S_o of 100 g/L. These results correlate with the definitions of K_1 and K_2 .

Table 4 - 3: Kinetic constants of the Peleg model; correlation coefficient (R^2), root mean square error (RMSE) for assessing adequacy of the model

| S_o (g/L) | E_o ($\mu\text{L/L}$) | K_1 | K_2 | R^2 | RMSE |
|-------------|---------------------------|-------|-------|--------|--------|
| 125 | 62 | 105.0 | 0.778 | 0.9822 | 0.0337 |
| 125 | 125 | 69.8 | 0.839 | 0.9915 | 0.0258 |
| 125 | 188 | 50.3 | 0.840 | 0.9828 | 0.041 |
| 125 | 250 | 26.2 | 0.837 | 0.9754 | 0.0568 |
| 100 | 125 | 53.7 | 0.745 | 0.9861 | 0.0387 |
| 125 | 125 | 69.7 | 0.839 | 0.9915 | 0.0258 |
| 150 | 125 | 82.9 | 0.893 | 0.9959 | 0.0158 |

It is observed that K_1 is proportional with S_o and inversely proportional with E_o . K_2 shows the opposite behavior. If the relationship between K_1 and K_2 and $E_o:S_o$ can be established, the $E_o:S_o$ ratio can be used to predict the K values.

Plotting K_1 and $E_0:S_0$ gives a good linear equation with a high R^2 of 0.97, Figure 4 - 5.

$$K_1 = -50.7 \times \frac{E_0}{S_0} + 123.95 \quad (4.4)$$

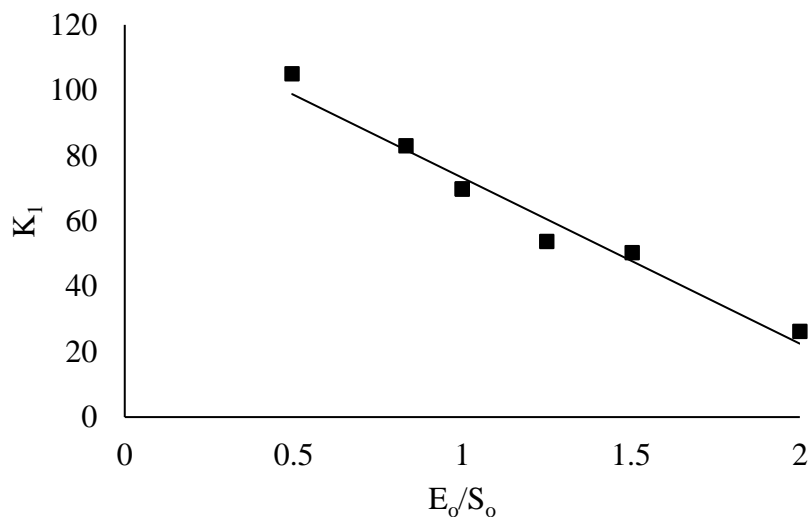


Figure 4 - 5: Variation of K_1 for different E_0/S_0 values

However, there is not a similar fit, linear or otherwise, between K_2 and $E_0:S_0$. As defined above, K_2 is Peleg's capacity constant relating to the maximum DM, but as noted above experiments with a low $E_0:S_0$ were not run for a long enough to reach the maximum DM. This will skew the values of K_2 .

4.2.2 The exponential equation

In order to see if a better fit could be obtained, the exponential equation was used. As discussed previously, this has been commonly used in the kinetic study of protein enzymatic hydrolysis [2].

$$DM = \frac{1}{b} \ln(1 + abt) \quad (4.5)$$

The fit of the exponential equation with the experimental data in this study is shown in Figure 4 - 7 and Figure 4 - 6.

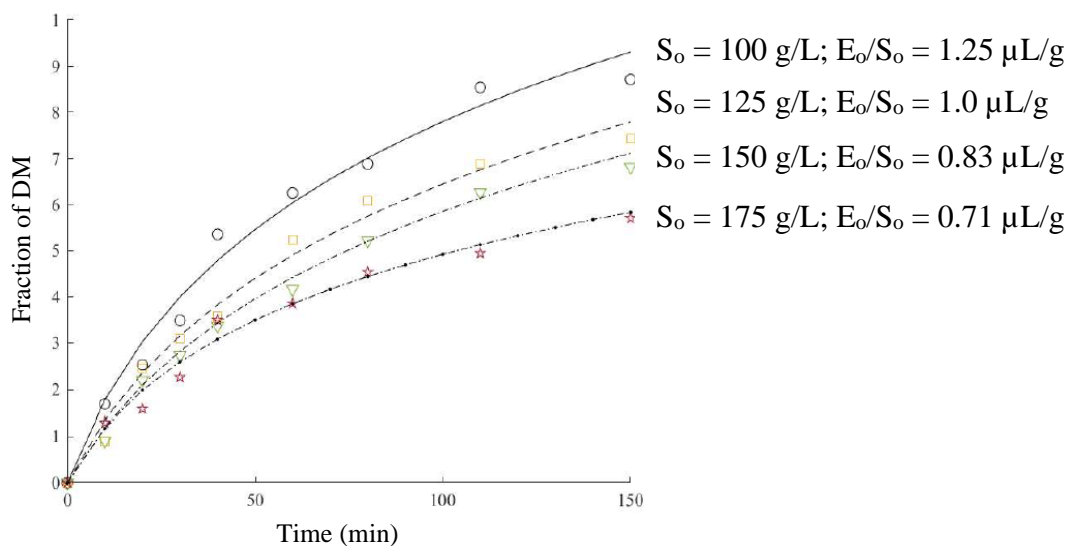


Figure 4 - 6: Kinetic curves for the fraction of DM. Symbols represent for experimental data; lines are the exponential model predictions. The initial substrate concentrations are indicated in the curves, $E_o = 125 \mu\text{L/L}$

The model fit the exponential model well, having all R^2 higher than 0.95, but the fit was not as good as the Peleg model. The values of kinetic parameters 'a' and 'b' corresponding to experiments conducted at different E_o and S_o are determined through non-linear regression analysis in accordance with the equation (4. 5), **Error! Not a valid bookmark self-reference..**

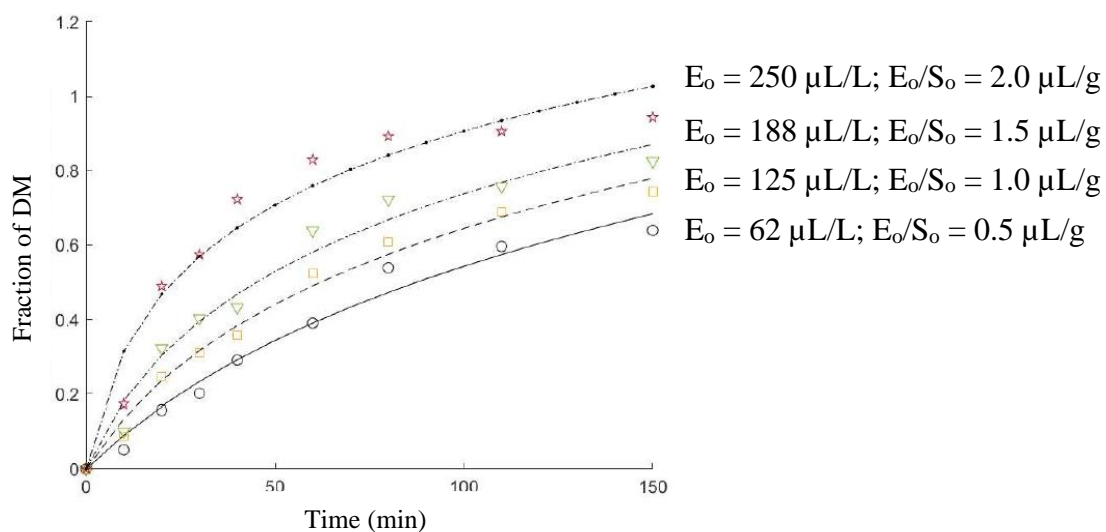


Figure 4 - 7: Kinetic curves for the fraction of DM. Symbols represent for experimental data; lines are the exponential model predictions. The initial enzyme concentrations are indicated in the curves. $S_0 = 125$ g/L

Table 4 - 4: Kinetic parameters 'a' and 'b' of the exponential model; correlation coefficient (R^2), root mean square error (RMSE) for assessing adequacy of the model.

| S_0 (g/L) | E_0 ($\mu\text{L/L}$) | a | b | R^2 | RMSE |
|-------------|---------------------------|-------|-------|--------|--------|
| 125 | 62 | 0.010 | 2.054 | 0.9787 | 0.0369 |
| 125 | 125 | 0.016 | 2.510 | 0.9875 | 0.0313 |
| 125 | 188 | 0.024 | 2.713 | 0.9756 | 0.0489 |
| 125 | 250 | 0.055 | 3.225 | 0.9546 | 0.0771 |
| 100 | 125 | 0.022 | 2.318 | 0.9819 | 0.0443 |
| 125 | 125 | 0.016 | 2.505 | 0.9876 | 0.0312 |

| | | | | | |
|-----|-----|-------|-------|--------|--------|
| 150 | 125 | 0.014 | 2.643 | 0.9951 | 0.0174 |
|-----|-----|-------|-------|--------|--------|

As discussed, and outlined in Table 2- 4, the relationship ‘a’ and ‘b’ to reaction rate constants (e.g., K_m) depends on a proposed mechanism if there is substrate and/or product inhibition.

In the case of parameter ‘a’, ‘a’ increases with decreasing S_o and increasing E_o . The good fit of ‘a’ with $E_o:S_o$ is linear, $R^2 > 0.85$, indicated in Figure 4 - 8. It matches with the behavior of ‘a’ in terms of a no inhibition mechanism [2].

$$a = 0.0286 \times \frac{E_o}{S_o} - 0.0106 \quad (4.6)$$

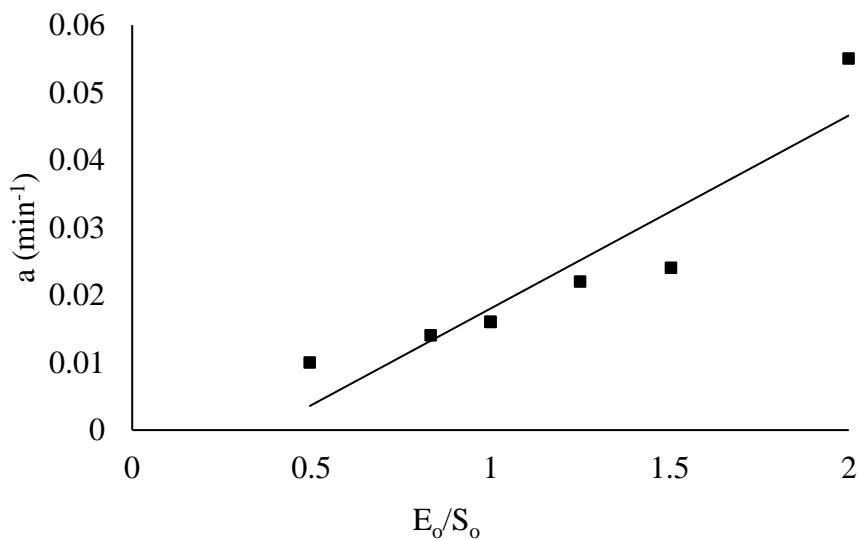


Figure 4 - 8: Variation of parameter ‘a’ for different E_o/S_o values

In theory, ‘b’ should be constant for the no inhibition mechanism and proportional to S_o for the other mechanisms outlined in Chapter 3 [2]. However, it is observed that “b”

increases with S_o . The lack of agreement between the trend in 'b' is potentially a result of our use of DM versus DH. DH reflects all peptide cleavages from peptide cleavages of insoluble proteins and cleavages of soluble proteins in the hydrolysate. In our work, DM considers only the initial peptide cleavages to insoluble proteins (mussel meat). As such, any inhibition by-products may not be captured in the measurement of DM, thereby impacting the determination of 'b'. This impacts the accurate determination of the constants used in scale-up. Although, the relation of parameter 'b' and $E_o:S_o$ could not be established, no inhibition mechanism is proposed because of the confident relation of parameter 'a' and $E_o:S_o$.

4.2.3 First-order kinetic equation

Again, given the limitations of the Peleg and exponential model, a first-order kinetic equation discussed in chapter three is used. The following equation can describe the increase in the DM:

$$DM = DM_{\infty}(1 - e^{-kt}) \quad (4. 7)$$

Where DM_{∞} is the value of DM for $t \rightarrow \infty$, k is the rate constant, and t is the time (min). The experimental data and the calculated data are compared in Figure 4 - 10 and **Error!**

Reference source not found..

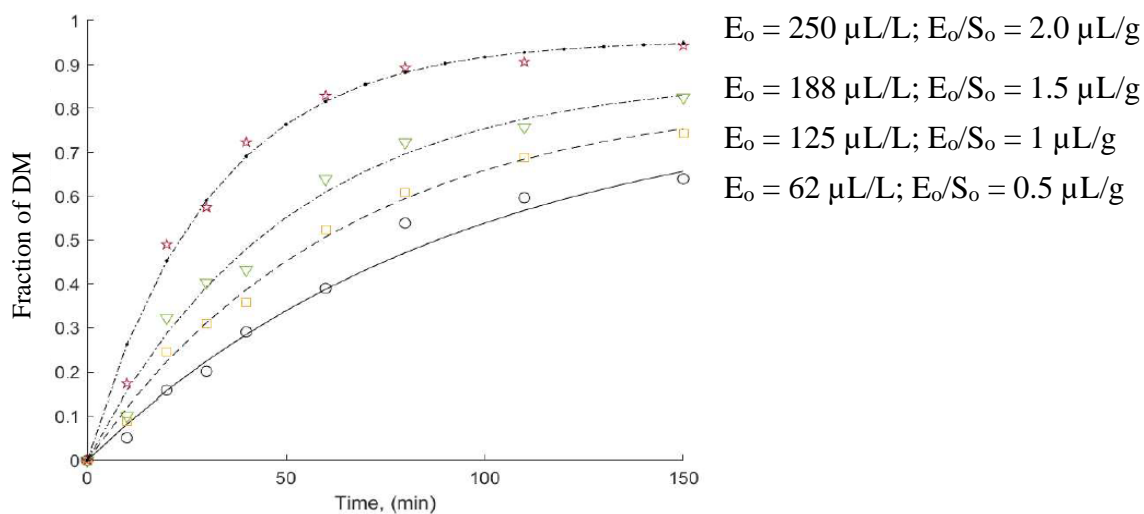


Figure 4 - 10: Kinetic curves for the fraction of DM. Symbols represent experimental data; lines are the first-order kinetic model prediction. The concentrations of the enzyme are indicated in the curves. $S_o = 125\text{g/L}$

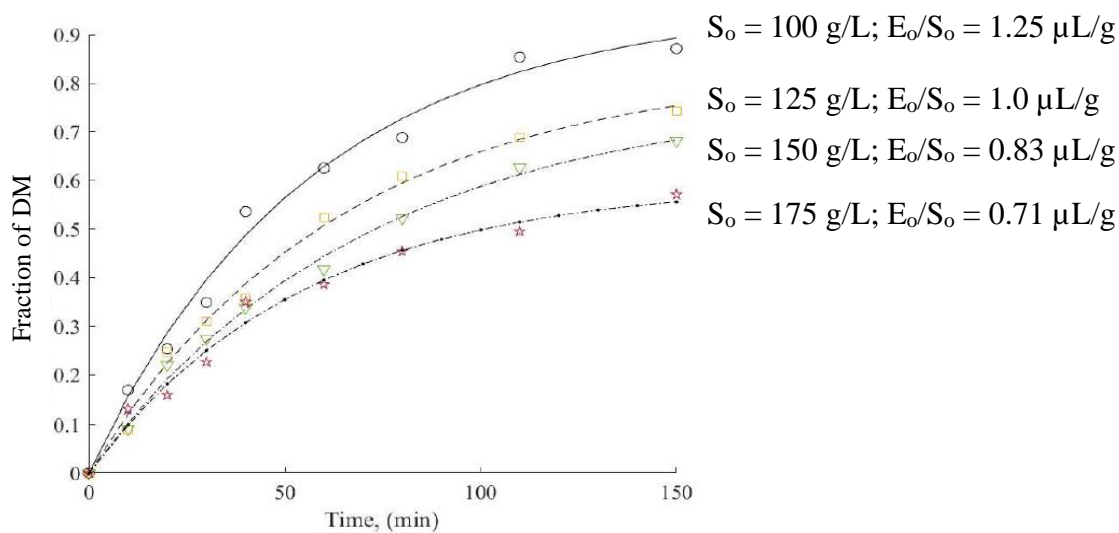


Figure 4 - 9: Kinetic curves for the fraction of DM. Symbols represent for experimental data; lines are the first-order model predictions. The types of mussel are indicated in the curves. $E_o = 125 \mu\text{L/L}$

The first-order equation showed a good fit to all experimental data, with the R^2 higher than the previous two models. DM_{∞} and kinetic constants k are estimated by non-linear regression,

Table 4 - 5.

Table 4 - 5: Kinetic constant and parameter of the first-order model, correlation coefficient (R^2), root mean square error (RMSE) for assessing adequacy of the model.

| S_0 (g/mL) | E_0 (μ L/mL) | DM_{∞} | $k \times 10^{-3}$ | R-square | RMSE |
|--------------|---------------------|---------------|--------------------|----------|---------|
| 125 | 62 | 0.825 | 11.06 | 0.9857 | 0.03024 |
| 125 | 125 | 0.834 | 15.63 | 0.9944 | 0.02099 |
| 125 | 188 | 0.873 | 19.98 | 0.9873 | 0.03531 |
| 125 | 250 | 0.956 | 32.12 | 0.9877 | 0.04018 |
| 100 | 125 | 0.960 | 17.33 | 0.9889 | 0.03468 |
| 125 | 125 | 0.834 | 15.63 | 0.9944 | 0.02100 |
| 150 | 125 | 0.777 | 14.12 | 0.9956 | 0.01659 |

As with the other models, correlating the k and DM_{∞} with $E_0:S_0$ is required for scale-up and reactor design. The rate constant k is proportional with the initial enzyme concentration and inversely proportional with substrate concentration. It matches with the definition of k as well as the theory of protein enzymatic hydrolysis. The relation of k and $E_0:S_0$ is described by an exponential equation (4. 8) with a $R^2 > 0.97$ and shown in **Error!**

$$k = 0.007389 * \exp \left[0.7204 * \left(\frac{E_0}{S_0} \right) \right] \quad (4. 8)$$

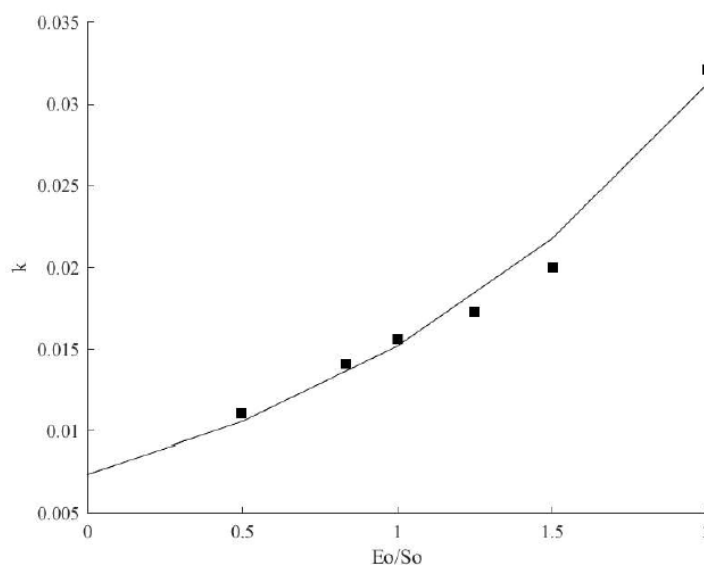


Figure 4 - 11: Variation of kinetic constant k for different E_0/S_0 values

Reference source not found..

DM_{∞} represents the maximum degree of digested meat. In this work, DM_{∞} is proportional to the initial enzyme concentration and inversely proportional with substrate concentration. This result is consistent with the theory of enzymatic hydrolysis of protein. However, the relationship of DM_{∞} and $E_0:S_0$ was inconsistent with respect to trend. This issue is similar

with the determination of parameter ‘b’ of exponential model where at low $E_o:S_o$ experiments were not run long enough to determine the maximum DM. The constant k is calculated where the rate is changing most significantly in the initial and mid point of experiments and therefore is not impacted.

It should be noted these experiments could not re-run for extended periods due to the covid pandemic but will be added for future work. However, in the initial screening studies early in the experimental work where E_o was varied, a run time of 210 min was used to optimize the sampling procedure. These experiments were not done in duplicate as they were only

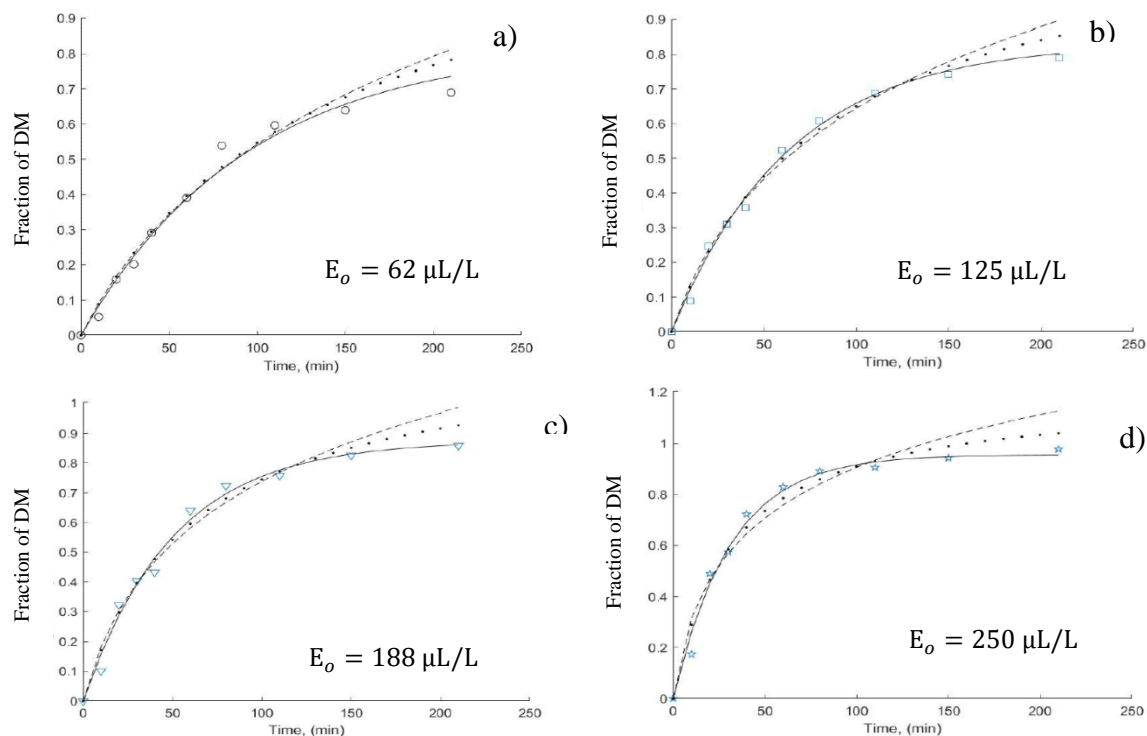


Figure 4 - 12: The fraction of DM as function of hydrolysis time. Symbols represent for experimental data; solid lines (—), dotted lines (···), and slanted lines (---) are the first-order kinetic model, Peleg model, and steady state model predictions, respectively. $S_o = 125\text{g/L}$

used for screening purposes and not in model development. However, they are useful to assess the model performance at longer times. The experimental results and models' prediction in period of 210 min are shown in Figure 4 - 12.

The first-order model predicts the steady state (maximum DM) for different initial enzyme concentration well, which trend to limit values, while the other models in this study continue to increase overshooting the experimental values.

In summary, the first-order model fits the experimental data very well. Under the experiment design of this study, the first-order model is suggested as the best model to describe as well as to predict the enzymatic hydrolysis of whole raw mussels.

4.3 Protein concentration of hydrolysate obtained from mussel meat hydrolysis

As mentioned above, the obtained hydrolysate could be a potential source of proteins. The soluble protein concentration quantitation is an integral part of any study involving protein hydrolysate such as analysis, separation, isolation, and recovery. Bio-Rad protein assay based on Bradford method is used to determine the concentration of soluble proteins of the obtained hydrolysate samples, and the results are shown in Table 4 - 6.

Table 4 - 6: Protein concentration of the obtained hydrolysate

| Sample No. | E_o ($\mu\text{L/L}$) | S_o (g/L) | DM | m_o (g) | Δm (g) | Protein Concentration (mg/L) |
|------------|------------------------------|---------------------------|-------|--------------|-------------------|---|
| (P-1) | 250 | 125 | 0.943 | 14.93 | 14.082 | 518.2 |

| | | | | | | |
|-------|-----|-----|-------|-------|--------|-------|
| (P-2) | 125 | 100 | 0.871 | 10.45 | 9.102 | 204.3 |
| (P-3) | 125 | 125 | 0.742 | 14.88 | 11.041 | 218.9 |
| (P-4) | 125 | 150 | 0.682 | 18.65 | 12.719 | 268.4 |
| (P-5) | 125 | 175 | 0.571 | 22.70 | 12.962 | 364.1 |

The soluble protein concentration is controlled by the initial enzyme concentration, the initial substrate concentration, and the size of mussels. The soluble protein concentration increases with the increase of the amount of digested meat. The hydrolysate with highest soluble protein concentration is obtained for sample (P-1), 5182 mg/mL. The results are consistent with the content of protein in mussel meat, approximately 14.5 wt% of protein in mussel wet meat [3].

However, in this study, the soluble protein concentration in the obtained hydrolysate solution cannot be directly compared to results in other studies. In other studies, the hydrolysis yield and the soluble protein content were based on freeze-dried hydrolysate [4]. However, it should be noted that freeze drying hydrolysate can impact the quality of the proteins and therefore both methods should be studied to compare yields and assess impact on protein profiles.

REFERENCES

- [1] J. E. Zapata Montoya, D. E. Giraldo-Rios, and A. J. Baéz-Suarez, “Kinetic modeling of the enzymatic hydrolysis of proteins of visceras from red tilapia (*Oreochromis sp.*): Effect of substrate and enzyme concentration,” *Vitae*, vol. 25, no. 1, pp. 17–25, 2018.
- [2] Q. Wei and H. Zhimin, “Enzymatic hydrolysis of protein : mechanism and kinetic model,” vol. 38, pp. 308–314, 2006.
- [3] L. Jönsson and K. Elwinger, “Mussel meal as a replacement for fish meal in feeds for organic poultry - a pilot short-term study,” *Acta Agric. Scand. A Anim. Sci.*, vol. 59, no. 1, pp. 22–27, 2009.
- [4] A. S. Naik, L. Mora, and M. Hayes, “Characterisation of seasonal *mytilus edulis* by-products and generation of bioactive hydrolysates,” *Appl. Sci.*, vol. 10, no. 19, pp. 1–21, 2020.

CHAPTER 5 – CONCLUSIONS AND RECOMMENDATIONS

5.1 Conclusions:

Development of green processes to valorize fisheries by-product is critical for the future sustainability of the industry as a whole. Blue mussel farming is a sustainable fishery with minimal impact on the environment. However, the mussel industry could further enhance its sustainability by recovering value from the processing by-product and reject mussels. Waste mussel shells are a rich source of bio-calcium carbonate and proteins. Enzymatic hydrolysis of waste mussel shells to value added products offers a simple and environmental-friendly process due to the mild operating conditions and zero waste streams. In this thesis, we used Multifect PR 6L to hydrolyze mussel meat of raw mussels. The literature review shows that waste mussel shells in general are underutilized and kinetics of the meat removal process by using enzymatic hydrolysis is not well studied. Mussel shells is primarily mineral rich, consisting largely of calcium carbonate (CaCO_3), which has been demonstrated to have a potential for various applications. Mussel meat in waste mussel shells is also a rich source of protein that could be exploited for fishmeal production.

In this study, the enzymatic hydrolysis of raw mussel was carried out by using Multifect PR 6L enzyme and ap water at temperature 50 °C and neutral pH. The initial concentration of substrate and enzyme was varied to evaluate effects the rate and extent of hydrolysis. The performance of hydrolysis process was measured using the degree of digested meat (DM) instead of the degree of hydrolysis (DH). Increasing initial enzyme concentration led

to an increasing rate and final DM while the increasing initial substrate concentration resulted in decreasing rate and DM. The higher the enzyme concentration the more sites for reaction, whereas higher initial substrate concentrations not only require more enzyme but also can limit mass transfer thereby slowing the rate of hydrolysis. The highest DM was obtained in these experiments at $E_o = 250 \mu\text{L/L}$ and $S_o = 125 \text{ g/L}$ or an $E_o:S_o$ of 2. A first-order kinetic model which assumed no inhibition and no autolysis of enzyme, was proposed to describe and predict the DM of the hydrolysis process with $R^2 > 0.98$. The rate constant can be predicted based on the $E_o:S_o$ ratio:

$$DM(t) = DM_{\infty} \left(1 - e^{-0.007389 \cdot \exp\left[0.7204 \cdot \left(\frac{E_o}{S_o}\right)\right] t} \right)$$

The concentration of soluble proteins in the obtained hydrolysate was measured by Bio-Rad protein assay based on Bradford method. The highest soluble protein concentration of 518.2 mg/L was obtained at $E_o = 250 \mu\text{L/L}$ and $S_o = 125 \text{ g/L}$. With these results, it could not be evaluated the potential of using the obtained hydrolysate for fishmeal production. However, this is a preliminary assessment for further analysis as well as the protein recovery.

5.2 Future Recommendations:

The actual mechanism of the hydrolysis of mussels would be useful to give a fuller picture of the rate. Future recommendations for this work are summarized as follows:

- Extend the experimental time of the hydrolysis process for very low $E_0:S_0$ to get a better estimate of the maximum DM (DM_∞). This will allow an equation to be developed to predict DM_∞ as a function of E_0 and S_0 .
- Perform experiments based on the optimal reaction conditions on broken mussels to confirm if the mass transfer and the adductor limit the reaction rate.
- The hydrolysate quality is a function of protein content and protein distribution. Many studies freeze dry the hydrolysate before analysis. This can impact the protein quality. As such, both the freeze dried and “wet” hydrolysate should be compared for protein distribution (amino acids).